



UNIVERSITEIT•STELLENBOSCH•UNIVERSITY
jou kennisvennoot • your knowledge partner

The limitations of a continuous wave Doppler radar for vehicle speed measurement and enforcement

Johann Ruben van Tonder
22569596

Report submitted in partial fulfilment of the requirements of the module
Project (E) 448 for the degree Baccalaureus in Engineering in the Department of
Electrical and Electronic Engineering at Stellenbosch University.

Supervisor: Dr W. Steyn

November 2022

Acknowledgements



UNIVERSITEIT•STELLENBOSCH•UNIVERSITY
jou kennisvennoot • your knowledge partner

Plagiaatverklaring / Plagiarism Declaration

1. Plagiaat is die oorneem en gebruik van die idees, materiaal en ander intellektuele eiendom van ander persone asof dit jou eie werk is.

Plagiarism is the use of ideas, material and other intellectual property of another's work and to present it as my own.

2. Ek erken dat die pleeg van plagiaat 'n strafbare oortreding is aangesien dit 'n vorm van diefstal is.

I agree that plagiarism is a punishable offence because it constitutes theft.

3. Ek verstaan ook dat direkte vertalings plagiaat is.

I also understand that direct translations are plagiarism.

4. Dienooreenkomsdig is alle aanhalings en bydraes vanuit enige bron (ingesluit die internet) volledig verwys (erken). Ek erken dat die woordelikse aanhaal van teks sonder aanhalingstekens (selfs al word die bron volledig erken) plagiaat is.

Accordingly all quotations and contributions from any source whatsoever (including the internet) have been cited fully. I understand that the reproduction of text without quotation marks (even when the source is cited) is plagiarism

5. Ek verklaar dat die werk in hierdie skryfstuk vervat, behalwe waar anders aangedui, my eie oorspronklike werk is en dat ek dit nie vantevore in die geheel of gedeeltelik ingehandig het vir bepunting in hierdie module/werkstuk of 'n ander module/werkstuk nie.

I declare that the work contained in this assignment, except where otherwise stated, is my original work and that I have not previously (in its entirety or in part) submitted it for grading in this module/assignment or another module/assignment.

Studentenommer / Student number	Handtekening / Signature
Voorletters en van / Initials and surname	Datum / Date

Abstract

English

Afrikaans

Contents

Declaration	ii
Abstract	iii
List of Figures	vii
List of Tables	ix
Nomenclature	x
1. Introduction	1
1.1. Background	1
1.2. Problem Statement	2
1.3. Objectives	2
1.4. Summary of Work	2
1.5. Scope	2
1.6. Format of Report	2
2. Literature Review	4
2.1. Proposed Doppler Radar Solutions	4
3. Radar Physics	6
3.1. Electromagnetic Wave Propagation	6
3.2. Radar Equation	7
3.3. Radar Frequencies	8
3.4. Radar Cross Section	9
3.5. CW Doppler Radar	10
3.6. Frequency Resolution	11
3.7. Range Resolution	12
3.8. Radar Clutter	13
3.9. Antenna Parameters	13
4. Limitations of a CW Doppler radar in Vehicle Speed Measurement	15
4.1. Cosine Effect	15
4.2. Accuracy and Acceleration Limits	16
4.3. Object Identification	17

4.4. Antenna Sidelobes	18
4.5. Multiple Path Reflection	19
4.6. Radar Receiver Saturation	19
5. Doppler Radar	21
5.1. System Design	21
5.1.1. Doppler Sensor	21
5.1.2. Antenna	22
5.1.3. Lowpass Filter and Amplifier	22
5.1.4. Voltage Regulator	22
5.1.5. Soundcard	23
5.1.6. Software	23
5.2. Detailed Design	23
5.2.1. Filter	23
5.2.2. Amplifier	24
5.2.3. Voltage Regulator	26
5.2.4. Clipper	26
5.2.5. Antenna	27
5.2.6. Software	29
6. Results	30
6.1. Radar and Setup	30
6.2. Radar Results	31
6.3. Limitations and Operation	32
6.3.1. Results of Cosine Effect	32
6.3.2. Results of Accuracy and Acceleration Limits	32
6.3.3. Results of Object Identification	34
6.3.4. Results of Antenna Sidelobes	34
6.3.5. Results of Multiple Path Reflection	34
6.3.6. Results of Radar Receiver Saturation	35
7. Conclusion	36
Bibliography	37
A. Project Planning Schedule	39
B. Outcomes Compliance	40
C. Figures	41
D. Radar Software	42

E. Antennas	44
F. LTSpice Simulations	45
G. Spectrogram regarding Accuracy and Acceleration	47
H. Spectrograms regarding Antenna Sidelobe	49

List of Figures

2.1. Proposed Doppler speed Measurement Configuration	4
3.1. Electromagnetic Waveform	6
3.2. A Basic Radar	7
3.3. Equivalent Sphere shape	9
3.4. CW Doppler Radar	11
3.5. Result of Frequency Mix	11
4.1. Cosine Angle β	15
4.2. Frequency Versus Time Resolution	16
4.3. Vehicle Ranges for Equal Echo Power	17
4.4. Antenna Radiation Pattern	18
4.5. Multiple Reflections	19
4.6. Intermodulation Distortion	20
5.1. System Diagram of Project	21
5.2. Patch Antenna on HB100	22
5.3. Horn Antenna	22
5.4. Functional Block diagram	22
5.5. Filter Circuit	24
5.6. Amplifier Circuit	25
5.7. Voltage Swing Circuit	26
5.8. Voltage Reference Circuit	26
5.9. Voltage Regulator Circuit	26
5.10. Diode Clipper Circuit	27
5.11. Rectangular Waveguide	28
5.12. Horn Geometry	28
6.1. Caption	30
6.2. Radar Setup	31
6.3. Spectrogram of Nissan X-trail traveling at 36 km/h	31
6.4. Speed Extraction from STFT	31
6.5. Cosine Error on Vehicle Speed	32
6.6. Measured Speed with best combination of Time and Frequency Differentiation	33
6.7. Measured Speed with Differentiation in Frequency	33

6.8. Measured Speed with Differentiation in Time	34
6.9. Spectrogram of Radar Receiver Saturation	35
6.10. Speed tracking when Saturation occurs	35
C.1. Gain versus Frequency plot of MCP602 op-amp	41
D.1. Signal-to-Noise Ratio	43
E.1. HB100 Radiation Pattern in CST	44
E.2. HB100 3D Radiation Pattern in CST	44
E.3. Schematic Drawing of HB100 Sensor	44
F.1. LTSpice Simulation of Radar Hardware	45
F.2. Input and Amplified Output	46
F.3. Frequency Response of Lowpass Filter	46
G.1. Spectrogram with best combination of Time and Frequency Resolution	47
G.2. Spectrogram with Differentiation in Frequency	47
G.3. Spectrogram with Differentiation in Time	48
H.1. Caption	49
H.2. Caption	49
H.3. Caption	50

List of Tables

2.1. Accuracy Comparison from HB100 Sensor	5
3.1. Standard Microwave Frequency letter-band nomenclature	8
3.2. Doppler Shift as a Function of Velocity and Frequency	12
4.1. Estimates of vehicle RCS	17
6.1. Measurable Distance of Radar	34

Nomenclature

Variables and functions

E	Electric
H	Magnetic
R	Range
G	Gain
V	Voltage
I	Current
P	Power
P_t	Transmitter Power
P_d	Power Density
σ	Radar Cross section
λ	Wavelength
A	Receive Aperture
τ	Dwell Time
c	Speed of light
τ_p	Pulse width
t_i	Measurement Time

Acronyms and abbreviations

RADAR	Radio Detection and Ranging
CSIR	Council for Scientific and Industrial Research
EV	Electrical Vehicle
PBY	Patrol Bomber Y
LiDAR	Light Detection and Ranging
CW	Continuous Wave
FMCW	Frequency Modulated Continuous Wave
RCS	Radar Cross Section
SNR	Signal to noise ratio
NBF	Narrow band filter
FFT	Fast Fourier transform
DFT	Discrete Fourier transform
STFT	Short time Fourier transform
RC	Resistor and Capacitor
ADC	Analog to Digital Converter
AGC	Automatic Gain Control
RMS	Root Mean Squared
GNSS	Global Navigation Satellite System
NMEA	National Marine Electronic Association
PC	Personal Computer
OP-AMP	Operational Amplifier
DC	Direct Current
AC	Alternating Current
LCD	Liquid-Crystal Display
SNR	Signal-To-Noise Ratio

Chapter 1

Introduction

1.1. Background

The traditional way of measuring vehicle speeds is done with the well-known phenomenon called the Doppler effect. Doppler radars were invented in the second world war, by John L. Barker Sr. and Ben Midlock [1]. They were tasked with solving the problem of terrestrial landing gear damage on the now legendary aircraft the PBY Catalina [2]. Barker and Midlock attached a Doppler radar unit, made out of coffee cans soldered shut to act as microwave resonators, to the end of the runway to measure the sink rate of landing PBYs. The radar gun was later used in 1947 by the Connecticut State Police in Glastonbury, Connecticut. After two years of testing and surveying in 1949, the state police began issuing speed tickets. Over the years the use of Doppler radar guns has come under some scrutiny. In 1987, the CSIR did their independent case study [3] on the validity of Doppler radars for vehicle speed measurements. The case study reported that there are several limitations in vehicle speed measurements, but most importantly the limitation that posed the greatest threat is identifying which vehicle is supplying the measurement. Knowing these limitations might limit the error in vehicle speed measurements and improve accuracy. Establishing how accurate Doppler radars are in vehicle speed measurements might give rise to a change in how vehicle speed is enforced. The goal is to increase safety on roads and limit accidents while making sure the right person is punished for speeding. Below are the operation parameter prescribed by law when using Continuous-Wave(CW) Doppler radars to measure vehicle speed in South Africa,

- No metal road signs or vertical flat surfaces larger than 1 meter in vertical height within 15° on either side of the aiming direction, within a distance of 200 m of the antenna.
- No signals received and processed from vehicles more than 500 meters away
- No other moving vehicle other than the measured vehicle within 600 metres from the radar in the direction of operation
- The vehicle's speed should be tracked for 3 s for a valid reading to be possible

1.2. Problem Statement

The problem I am tasked with is to investigate possible limitations in vehicle speed measurements and enforcements when using a CW Doppler radar. The objective of the report is to determine the limitations of a CW Doppler radar and if the prescribed operating laws are sufficient in mitigating the limitations in vehicle speed measurement.

1.3. Objectives

- Identify the possible limitations of CW Doppler radars in vehicle speed measurements
- Develop hardware for a CW Doppler radar that can perform up to 80 m
- Develop software capable of calculating the speed of targets
- Develop software capable of tracking a vehicle
- The radar should be able to distinguish between a vehicle and clutter
- Test the system under the specified laws and regulations standards for speed measuring
- Test the theorized limitations of CW Doppler limitations in vehicle speed measurements
- Conclude on whether the laws and regulations are satisfactory in limiting possible errors and limitations

1.4. Summary of Work

1.5. Scope

1.6. Format of Report

- **Chapter 1** introduces important information used to formulate the problem. The objectives for the report are mentioned followed by a reflection on what objectives were successfully executed. The chapter then discusses the scope of work that was not considered and what important limitations were not included in the report.
- **Chapter 2** discusses other notable work on Doppler radars and their application to vehicle speed measurements. This is also where I pointed out how my report differs from previous work.

- **Chapter 3** starts with the introduction to radar physics and what concepts allow radars to work. I then go on to explain the important fundamentals of radars that a reader of this report should know.
- **Chapter 4** formulates the limitations of Doppler radars in vehicle speed measurement.
- **Chapter 5** is where I discuss how I built a Doppler radar that I used to test the formulated limitations. This includes hardware and software design and development.
- **Chapter 6** starts with a formulation of how I tested the CW Doppler radar. I then discuss how the tests were constructed to test the limitations formulated in Chapter 4. I end the chapter by comparing the results from different tests and designs.
- **Chapter 7** concludes the report and points to possible future work.

Chapter 2

Literature Review

2.1. Proposed Doppler Radar Solutions

A proposed solution to the problem of vehicle identification was developed by Neil Cameron Martin [4] published in 1987, where the proposed system shown in Figure 2.1, indicates the use of two sources to measure and compare their results. For example, source one only measures vehicle speeds of B and C and source two only measures vehicle speeds of A and C. The configuration will allow you to determine which vehicle is travelling at what speed. The thesis concluded that the system improved the reliability of identifying which vehicle is travelling at what speed. Unfortunately, this system has not been adopted into law enforcement speed regulations. Leaving the case study of the CSIR still at the heart of the problem. This might be due to the complex real-time processing required at the time to successfully implement the system.

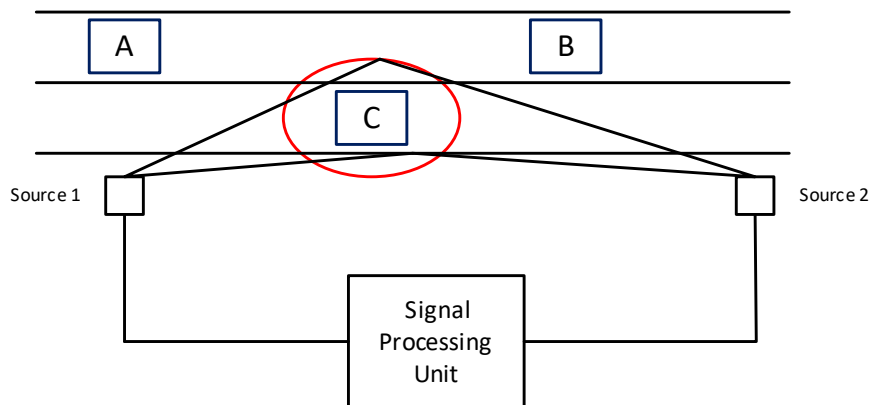


Figure 2.1: Proposed Doppler speed Measurement Configuration

Other noteworthy work was done by Nguyen Giang Lam [5]. Nguyen focussed on developing a Doppler radar with an HB100 X-band sensor [6]. To quite some success Nguyen developed the sensor with an ESP-32 microcontroller module. The developed system was capable of measuring speeds close to the speed measured from the vehicle, shown in Table 2.1. Nguyen's work focused on building a functional Doppler radar and he did not focus on the limitations of a Doppler radar.

Table 2.1: Accuracy Comparison from HB100 Sensor

Speed from the car	Speed from the HB100 Sensor
0 Km/h	0 Km/h
10 Km/h	11 Km/h
17 Km/h	16 Km/h
20 Km/h	20 Km/h
25 Km/h	24 Km/h
30 Km/h	31 Km/h
35 Km/h	35 Km/h

Apart from the CSIR case study, there is very little information on how big an influence certain limitations of a Doppler radar have on vehicle speed measurements. In my project, I will aim to adapt the system design by Nguyen and instead of real-time processing I will instead focus on recording data and then applying different processing methods to indicate the formulated limitations, discussed in Chapter 4.

Chapter 3

Radar Physics

3.1. Electromagnetic Wave Propagation

The principle that allows radars to work stems from Maxwell's equation. Maxwell derived his electromagnetic wave equation from the corrected Ampère's circuit law shown in equation 3.1 and 3.2. Faraday's law of induction is shown in equation 3.3 and 3.4.

$$\nabla \cdot E = 0 \quad (3.1) \qquad \nabla \times E = -\frac{\partial B}{\partial t} \quad (3.2)$$

$$\nabla \cdot B = 0 \quad (3.3) \qquad \nabla \times B = \mu\epsilon \frac{\partial E}{\partial t} \quad (3.4)$$

Maxwell derivation is today replaced by combining Ampère's and Faraday's to obtain the electromagnetic wave equation in a vacuum shown in equation 3.5 and 3.6, known as the wave equation.

$$\frac{1}{\sqrt{\mu\epsilon}} \frac{\partial^2 E}{\partial t^2} - \nabla^2 E = 0 \quad (3.5) \qquad \frac{1}{\sqrt{\mu\epsilon}} \frac{\partial^2 B}{\partial t^2} - \nabla^2 B = 0 \quad (3.6)$$

The electromagnetic waveform is generated by a periodic change in the current inside an antenna. The waveform that is generated from the antenna is indicated in Figure 3.1, the blue waveform is the E-field, which is perpendicular to the red waveform, which is the H-field. The waveform propagates in the z-direction.

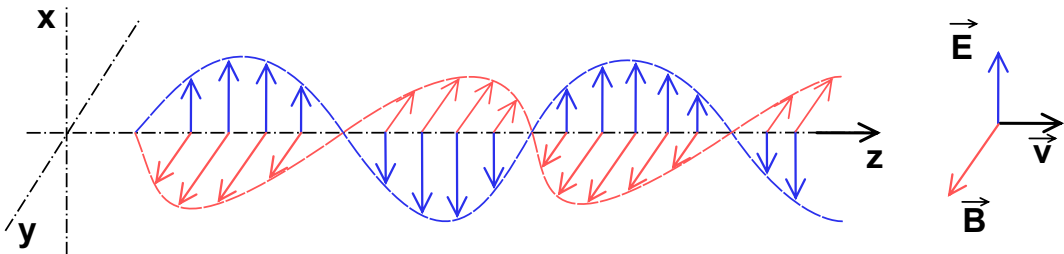


Figure 3.1: Electromagnetic Waveform

Consider the basic radar illustrated in Figure 3.2, it is an antenna transmitting an electromagnetic wave, the waveform then propagates through the air until it reaches a target. A portion of the transmitted energy is intercepted by the target and is scattered, some of it in the direction of the radar, where it is collected by the receiving antenna.

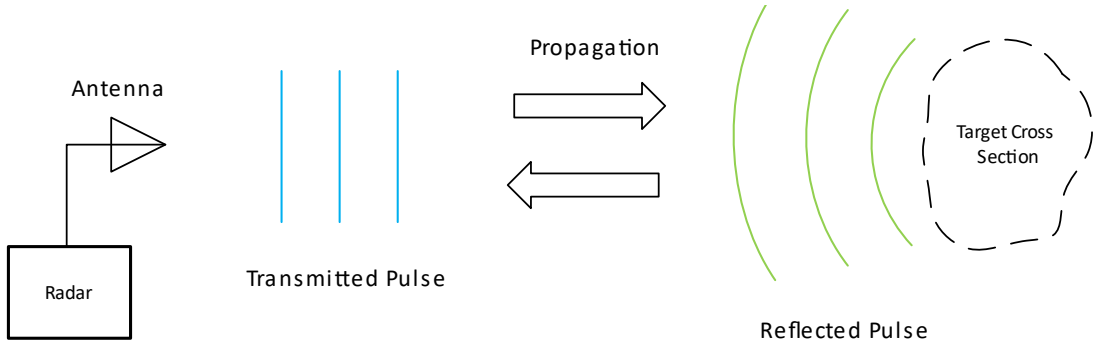


Figure 3.2: A Basic Radar

3.2. Radar Equation

The radar equation relates the range of radar to the characteristics of the transmitter, receiver, antenna, target and environment [7]. Understanding the radar equation not only gives you a means for determining the maximum distance from the radar to the target but can also serve as a tool for understanding radar operation and radar design. If the power of the radar transmitter is denoted by P_t , and if an isotropic antenna [8], one which radiates uniformly in all directions, is used. The power density P_d at a distance R from the radar is equal to the transmitter power divided by the surface area $4\pi R^2$ of an imaginary sphere of radius R , the power density is given by

$$P_d = \frac{P_t}{4\pi R^2} \quad (3.7)$$

When the radar employs a directive antenna to channel or direct the radiated P_t into some particular direction. The gain G of an antenna is a measure of the increased power radiated in the direction of the target as compared with the power that would have been radiated from an isotropic antenna. This means P_d at the target from an antenna with transmitting gain G is

$$P_d = \frac{P_t G}{4\pi R^2} \quad (3.8)$$

A portion of the radiated power is intercepted by the target and reradiated in various directions. The measure of the amount of incident power intercepted by the target and reradiated back towards the radar is denoted by the radar cross section σ , and is defined by the relation

$$P_d = \frac{P_t G}{4\pi R^2} \frac{\sigma}{4\pi R^2} \quad (3.9)$$

The radar cross-section σ has units of area. It is a characteristic of the particular target and is a measure of its size as seen by the radar. The radar antenna captures a portion of

the echo power. If the effect is denoted by A_e , the power P_r , received by the radar is

$$P_r = \frac{PtGA_e\sigma}{(4\pi)^2 R^4} \quad (3.10)$$

The maximum range of the radar R_{max} is the distance beyond which the target cannot be detected. It occurs when the received signal power P_r , just equals the minimum detectable signal S_{min} . Therefore

$$R_{max} = \left(\frac{PtGA_e\sigma}{(4\pi)^2 S_{min}} \right)^{\frac{1}{4}} \quad (3.11)$$

Antenna theory gives the relationship between the transmitting gain and the receiving effective area of an antenna as

$$G = \frac{4\pi A_e}{\lambda^2} \quad (3.12)$$

Generally, radars use the same antenna for transmitting and receiving by substituting equation 3.12 into equation 3.11, resulting in

$$R_{max} = \left(\frac{Pt(A_e)^2 \sigma}{4\pi(\lambda)^2 S_{min}} \right)^{\frac{1}{4}} \quad (3.13)$$

3.3. Radar Frequencies

Radar conventionally operate at frequencies from 220 MHz to 35 GHZ. These are not limits but rather standards proposed by the International Telecommunications Union [9]. Early in the development of radar, a letter code such as S, X, L, etc., was employed to designate radar frequency bands. The original purpose was to safeguard military secrecy, and the designation was maintained. The frequency band of importance for a Doppler radar are referred to as the Microwave region. The Microwave region ranges from 300MHz to about 36 GHz. Table 6.1 shows the designated bands inside the Microwave region.

Table 3.1: Standard Microwave Frequency letter-band nomenclature

Band Designation	Nominal Frequency range (GHz)
<i>UHF</i>	0.3-1
<i>L</i>	1-2
<i>S</i>	2-4
<i>C</i>	4-8
<i>X</i>	8-12
<i>K_u</i>	12-18
<i>K</i>	18-27

Doppler radars are operated in the *X*-band region, this is mainly due to law enforcement from the mid-1950s [10]. The reason behind using *X*-band as opposed to *K*-band or *K_u*-band is due to *X*-band being less affected by poor weather conditions. There are however disadvantages when using *X*-band over *K*-band, *X*-band requires a larger antenna and is easy for radar detectors to pick up at long distances. The reason for this is due to the wavelength

$$\lambda = \frac{c}{f} \quad (3.14)$$

The higher the frequency, the smaller the wavelength. Meaning the radar will be able to measure smaller details the higher its operating frequency is.

3.4. Radar Cross Section

The radar cross-section (RCS) [11], is a measure of the reflectivity of an object and is formulated as

$$\sigma = \lim_{R \rightarrow \infty} 4\pi R^2 \frac{I_r}{I_i} \quad (3.15)$$

where I_r is the reflected intensity and I_i is the incident intensity. The $4\pi R^2$, comes from the assumption, that the radar cross-section is assumed to take the shape of a sphere, this assumption is illustrated below

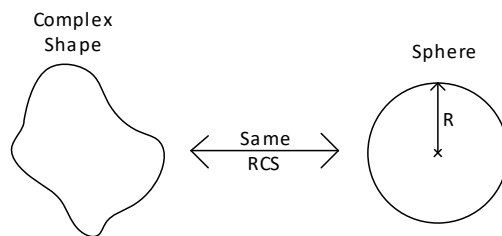


Figure 3.3: Equivalent Sphere shape

Most of the incident energy is scattered and only a small fraction is reflected on the radar. Larger objects usually, but not always, have larger reflections and a longer radar detection range R . The object parameters that influence the RCS are size, shape and reflectivity [12]. Flat surfaces reflect energy better than contoured shapes. Edges with diameters on the order of a wavelength of the radar frequency tend to be good reflectors. All metals and alloys are excellent reflectors at all frequencies. Metal screens with gaps spacing less than a quarter wavelength are as reflective as solid surfaces. Composites, fibreglass and plastic are bad reflectors at microwave frequencies.

3.5. CW Doppler Radar

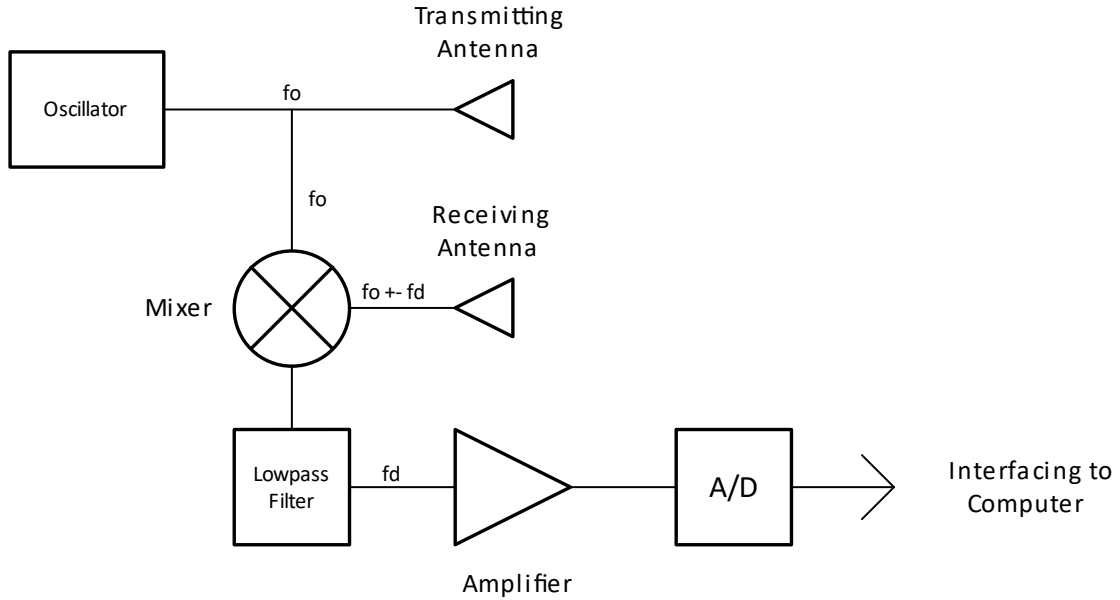
It is well known in the fields of optics and acoustics that if either the source of oscillation or the observer of the oscillation is in motion, an apparent frequency shift will result. This is known as the Doppler Effect and is the basis of CW Doppler Radar [7]. If the distance between the radar and target is R , the total number of wavelengths λ contained in the two-way path between the radar and target is $\frac{2R}{\lambda}$. Since one wavelength corresponds to an angular excursion of 2π radians, the total angular excursion ϕ made by the electromagnetic wave during its transit to and from the target is $\frac{4\pi R}{\lambda}$ radians. If the target is in motion, R and the phase ϕ are continually changing. A change in ϕ with respect to time is equal to a frequency. This is the Doppler angular frequency ω , given by equation 3.16

$$2\pi f_d = \omega = \frac{4\pi \partial R}{\partial t} = \frac{4\pi v}{\lambda} \quad (3.16)$$

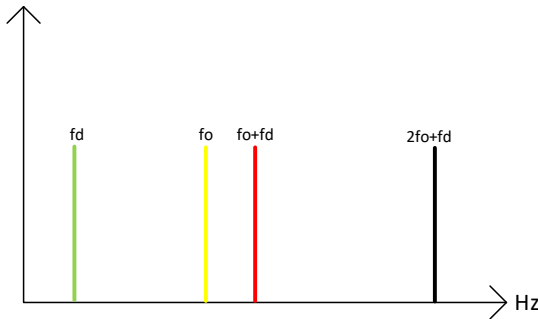
where f_d = Doppler frequency shift and v = relative velocity of target with respect to radar. The Doppler frequency shift is given by equation 3.17

$$f_d = \frac{2v}{\lambda} = \frac{2vf_o}{c} \quad (3.17)$$

where c is the speed of light in a vacuum. Consider the CW Doppler radar as illustrated in Figure 3.4. The oscillator generates a continuous frequency f_d , which is transmitted by the antenna. If the target is in motion with velocity v , relative to the radar, the received signal will be shifted in frequency from the transmitted frequency f_o , by an amount $\pm f_d$, given by equation 3.17. The plus sign associated with the Doppler frequency applies if the distance between the radar and target decreases. The minus sign applies if the distance is increasing. The received echo signal at frequency $f_o \pm f_d$, enters the radar via the antenna and is heterodyned in the mixer, with the transmitted signal f_o to produce a Doppler beat note of frequency f_d . This is illustrated in Figure 3.5, note that the sign of f_d is lost in the process.

**Figure 3.4:** CW Doppler Radar

The resulting Doppler frequency obtained from the mixer is then passed through a lowpass filter, to filter out all the frequency components above f_d . The signal is then amplified before its sampled by an analogue-to-digital converter and then passed on to the computer interface for signal processing and analysis.

**Figure 3.5:** Result of Frequency Mix

3.6. Frequency Resolution

Doppler frequency resolution is the ability to distinguish between two objects travelling at different speeds, but at the same distance from the radar. Frequency resolution is inversely related to the dwell time, the time an antenna spends on a target. The greater the dwell time the finer the frequency resolution

$$\Delta f_D = \frac{1}{\tau} \quad (3.18)$$

We can also estimate the Doppler accuracy as, where SNR is the signal to noise ratio

$$\delta f_D = \frac{\Delta f_D}{t\sqrt{2SNR}} \quad (3.19)$$

To plot the spectrum of the sampled signal individual narrow band filters(NBF) must be as narrow as possible in bandwidth to allow accurate Doppler measurements and minimize the amount of noise power. In theory, the operating bandwidth of a CW Doppler radar is infinitesimal. However systems with infinitesimal bandwidths cannot physically exist and thus, the bandwidth of CW Doppler radars is assumed to correspond to that of a gated CW waveform.

An NBF bank can be implemented using a Fast Fourier Transform(FFT). If the Doppler filter bank is implemented using FFT of size N_f , and if the individual NBF bandwidth is Δf_D , then the effective radar Doppler bandwidth is

$$B = N_f \Delta f_D \quad (3.20)$$

The table 3.2 below indicates the Doppler shift as a function of velocity and frequency [13].

Table 3.2: Doppler Shift as a Function of Velocity and Frequency

<i>f</i>		Doppler Shift f_D (Hz)	
Band	Frequency (GHz)	1 m/s	1km/h
<i>L</i>	1	6.67	4.8
<i>S</i>	3	20	14.39
<i>C</i>	5	33.3	23.99
<i>X</i>	10	66.7	47.98
<i>K_u</i>	16	107	76.797
<i>K_a</i>	35	233	167.44

3.7. Range Resolution

The range resolution of a radar is its ability to distinguish between two or more targets on the same bearing, the angle measured relative to a hypothetical north, but at different ranges [14]. The degree of range resolution depends on the width of the transmitted pulse τ_p , the types and sizes of targets, and the efficiency of the receiver. Pulse width τ_p is the primary factor in range resolution. The simplified theoretical range resolution can be calculated from

$$S_r = \frac{c\tau_p}{2} \quad (3.21)$$

An unmodulated CW Doppler radar does not have range resolution. To acquire range resolution some sort of timing mark must be applied to a CW carrier if the range is to be measured. The timing mark permits the time of transmission and the time of return to be recognized. The more distinct the mark, the broader the transmitted spectrum will be. This follows from the properties of the Fourier transform,

$$\mathfrak{F}(h(t)) = \int_{-\infty}^{\infty} h(t) e^{-j2\pi f_t t} dt \quad (3.22)$$

therefore a finite spectrum must be transmitted if transmit time or range is to be measured. The spectrum of a CW transmission can be broadened by the application of modulation either amplitude, frequency or phase. A widely used technique is to frequency-modulate the carrier resulting in a Frequency Modulated Continuous-Wave(FMCW).

3.8. Radar Clutter

Land clutter is difficult to quantify and classify. The clutter is widely dependent on the type of terrain, as described by its roughness and dielectric properties. Buildings, towers, and other structures give more intense echo signals than forests and vegetation because of the presence of flat reflecting surfaces. Land clutter will mostly affect the targets with small radar cross-sections, like motorcycles. Birds flying past a radar are also seen as a type of clutter.

3.9. Antenna Parameters

The purpose of the radar antenna is to act as a transducer between free-space propagation and guided-wave (transmission-line) propagation. The function of the antenna during transmission is to concentrate the radiated energy into a shaped beam which points in the desired direction in space. On reception, the antenna collects the energy contained in the echo signal and delivers it to the receiver. Antenna design and theory are very complex. To understand the application of an antenna in radars there are two pieces of theory to understand, namely Gain and Directivity.

Gain is a measure of the ability of the antenna to direct the power delivered to the input into radiation in a particular direction. Gain is measured at the peak radiation intensity. Consider the power density radiated by an isotropic antenna at a distance R and input power P_0 :

$$S = \frac{P_0}{4\pi R^2} \quad (3.23)$$

As isotropic antenna radiates equally in all directions and the power density S is found by dividing the radiated power by the area of the sphere with radius R . The isotropic

radiator is considered to be 100% efficient. The gain of a real antenna increases the power density in the direction of the peak radiation.

$$S = \frac{P_0 G}{4\pi R^2} \quad (3.24)$$

Directivity is a measure of the concentration of the radiation in the direction of the maximum. Directivity is the maximum radiation intensity over the average radiation intensity:

$$\text{Directivity} = \frac{U_{max}}{U_{avg}} \quad (3.25)$$

Directivity and gain differ only by efficiency, but the directivity is easily estimated from patterns. Gain, directivity times efficiency, must be measured. The average radiation intensity can be found from a surface integral on the radiation sphere of the radiation intensity divided by 4π , the area of a sphere in steradians.

$$U_{avg} = \frac{1}{4\pi} \int_0^{2\pi} \int_0^\pi U(\theta, \phi) \sin\theta d\theta d\phi \quad (3.26)$$

Chapter 4

Limitations of a CW Doppler radar in Vehicle Speed Measurement

4.1. Cosine Effect

The incorrect Doppler frequency is read from the radar when the vehicle is not travelling directly towards the radar, this is illustrated in figure 4.1. The phenomenon is called the Cosine Effect because the measured speed is directly related to the cosine angle between the radar and the vehicle's direction of travel. The cosine angle is calculated by the equation below,

$$\beta = \tan^{-1}\left(\frac{d}{R}\right) \quad (4.1)$$

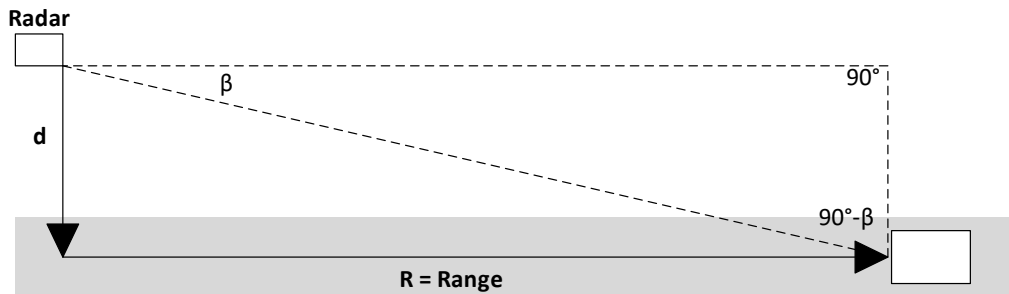


Figure 4.1: Cosine Angle β

The error in speed measurement is calculated in equation 4.2, where β is the angle of incident, R target range to radar and d is the antenna distance to the middle of the target lane. For this example, I only considered a straight lane in which the target travels and the radar is placed on the ground. As the target lane becomes curved or the radar is placed in the air the change in angle is too great for the radar to give an accurate result.

$$V_m = V_o \cos(\beta) = V_o \frac{R}{(R^2 + d^2)^{0.5}} \quad (4.2)$$

As highlighted in section 3.7 the CW Doppler radar cannot determine how far away a target is from the radar. There are some software techniques you can apply, but their

accuracy is questionable. The measured speed will always be less than the actual speed and thus care should be taken when enforcing minimum speed limits.

4.2. Accuracy and Acceleration Limits

Under ideal conditions, most speed measurement radars should have an accurate reading of about ± 1 km/h. A very important part of radar is to discriminate between different frequency components in a signal, in a short period. Radars are capable of extracting frequency from the measured values of an Analog-To-Digital Conversion(ADC) by a Discrete Fourier Transform(DFT) analysis of nonstationary signals. Nonstationary signals are signals that differ in frequency over time. To differentiate between frequency components a short period of the signal is used to calculate the frequency spectrum, hence the name Short Time Fourier Transform(STFT). The sample taken in the time domain has a trade-off in the frequency domain. To understand this trade-off you need to understand how the DFT works. The equation below shows how the DFT is calculated.

$$H[k] = \sum_{n=0}^{N-1} h[n]e^{-j2\pi kn/N} \quad (4.3)$$

The DFT takes a finite amount of samples, N , to calculate the frequency spectrum of discrete signal h . To increase the resolution of the frequency spectrum one can increase either the sampling frequency or the sampling period. Both methods have trade-offs, increasing the sampling frequency increases the processing power required to calculate the DFT in real time and by increasing the size of the sample you are decreasing the resolution in the time domain. The results of a DFT are represented in a spectrogram, which has time displayed on the horizontal axis, frequency on the vertical axis and spectral magnitude displayed on the third axis by colour. Figure 4.2 illustrates the trade-off between time and frequency, the first graph highlights how to differentiate between frequency components you will lose the ability in the time domain. The right-sided graph demonstrates the opposite, to differentiate in time you lose the ability to differentiate in the frequency domain.

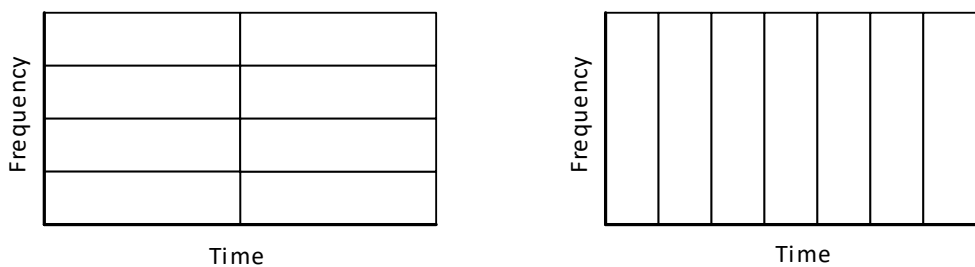


Figure 4.2: Frequency Versus Time Resolution

4.3. Object Identification

A CW Doppler radar uses the frequency spectrum to identify objects. As shown in Table 3.2, the frequency shift measured is a direct indication of how fast an object is moving. This is a very sound method and is capable of very accurate measurements. There is a problem nonetheless, how does the radar identify which object is travelling at what speed? For the case of a CW Doppler radar which does not have range resolution, discussed in section 3.7. A CW Doppler radar cannot distinguish between multiple vehicles/objects travelling at different speeds, both in the range of the radar. Due to Automatic Gain Control(AGC) being applied to the measured signal frequencies, the assumption of the closest object will generate the strongest signal is not true.

In Table 4.1 the estimate of vehicle RCS is illustrated. For motorists their RCS is relatively small, the motorcycle RCS normalised to a full-size pickup is 0.05 m^2 . This means that a motorcycle is very likely to be mistaken for a more distant vehicle. Figure 4.3, illustrates this phenomenon.

Table 4.1: Estimates of vehicle RCS

Vehicle Type	Radar Cross Section
Recreation Vehicle	400 m^2
Full Size Pickup	200 m^2
Large Car	120 m^2
Medium Size Car	60 m^2
Small Car	30 m^2
Motorcycle	10 m^2
Bicycle	5 m^2

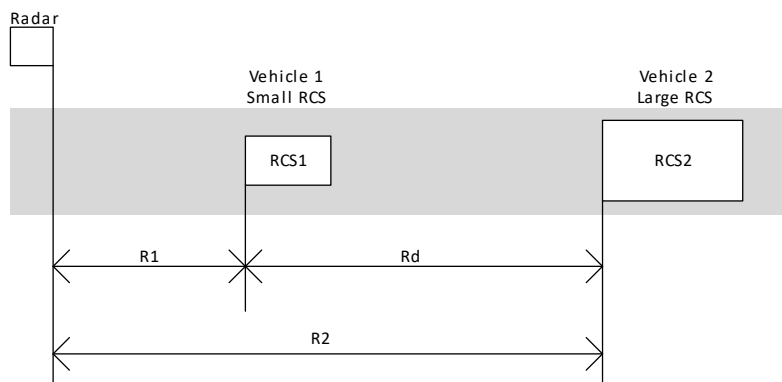


Figure 4.3: Vehicle Ranges for Equal Echo Power

The distance from the radar to the vehicle where the reflected power of vehicle two is equal to the reflected power of vehicle one, can be calculated by

$$R2 = R1 \left(\frac{\sigma_2}{\sigma_1} \right)^{\frac{1}{4}} \quad (4.4)$$

The equation can be written in terms if the distance between the two vehicles Rd ,

$$Rd = R1 \left[\left(\frac{\sigma_2}{\sigma_1} \right)^{\frac{1}{4}} - 1 \right] \quad (4.5)$$

Not only will the radar struggle to distinguish the travelling speeds of multiple vehicles in its range but it would also not be able to detect what the object is, that recorded the speed measurement. For instance, birds flying past the radar may cause false speed readings. This is not a likely phenomenon if it is just one bird due to a bird's RCS being usually around 0.1 m^2 . But when a swarm of birds fly past a radar it will cause the radar to have a false reading.

4.4. Antenna Sidelobes

An Antenna radiation pattern is a visual representation of the radiation emission from an antenna. Figure 4.4 shows how this can be plotted in polar coordinates. The main lobe is directed in the direction of the intended measurement. The side lobes are relatively small compared to the main lobe. This specific antenna's radiation pattern is very good to measure only in one direction. This is not always the case, some antennas might have very big side lobes. This will cause the radar to measure unintended objects that are not in the direction of measurement. Attention should be applied to the antenna radiation pattern when operating the radar.

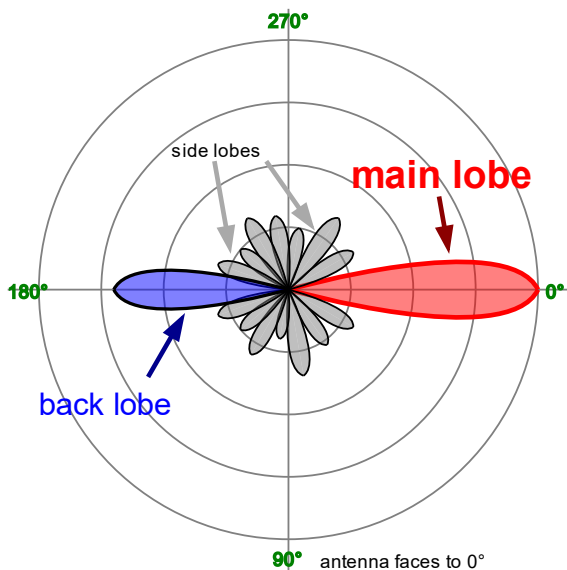


Figure 4.4: Antenna Radiation Pattern

Looking at the antenna radiation pattern of the HB100 sensor shown in figure ??,

the antenna is not very directional. When applying AGC, which is later explained in detail in section 5.1.3, to the received signals, it further complicates the process. This adds to the confusion of not knowing what object is reflecting what signal. Combining antenna radiation, side lobes, and AGC. It can compromise the credibility of a radar. It is important to know the radiation pattern of your radar for both the transmitting and receiving antenna otherwise, you will not be able to have accurate readings.

4.5. Multiple Path Reflection

The transmitted signal does not always take a direct path from radar to target and back. Any metal object, which is a good reflector, may lead to another path of reflection for the radar to measure. The radar is not capable of detecting how a signal has travelled from and back to the radar. A common object like an overhead or off-road highway sign can cause signals to reflect in multiple ways. Figure 4.5 shows two reflection paths the radar will measure when an overhead sign is placed on a highway.

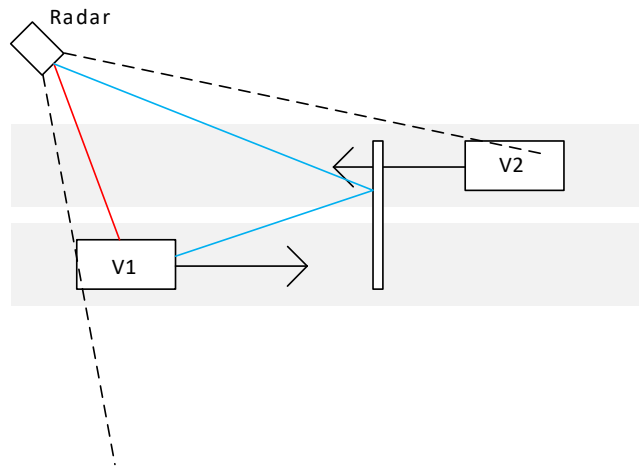


Figure 4.5: Multiple Reflections

The above illustration is just one example. There are more examples that are not as easy to quantify.

4.6. Radar Receiver Saturation

Strong echoes from larger vehicles close to the radar will reduce the radar detection range. The receiver will saturate and will not be able to measure any other vehicles in the radar range. Strong signals that saturate the radar receiver's low noise amplifier or mixer will produce cross-modulation products. Cross modulation, also known as intermodulation, is the amplitude modulation of signals containing two or more different frequencies. The intermodulation between frequency components will result in additional components at

frequencies that are not just at harmonic frequencies but also the sum and difference frequencies of multiples of those frequencies. Figure 4.6 illustrates how intermodulation can result in distortion and how this might saturate the radar receiver.

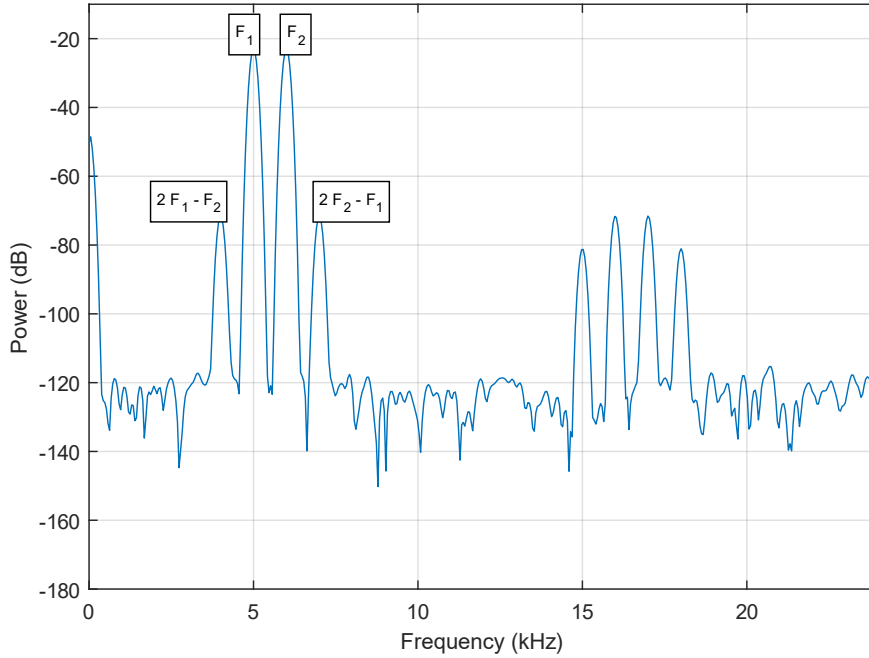


Figure 4.6: Intermodulation Distortion

To combat this some radars are equipped with AGC, to protect the receiver from signal saturation. The AGC reduces radar sensitivity but as mentioned in section 4.4 causes other problems to arise.

Chapter 5

Doppler Radar

5.1. System Design

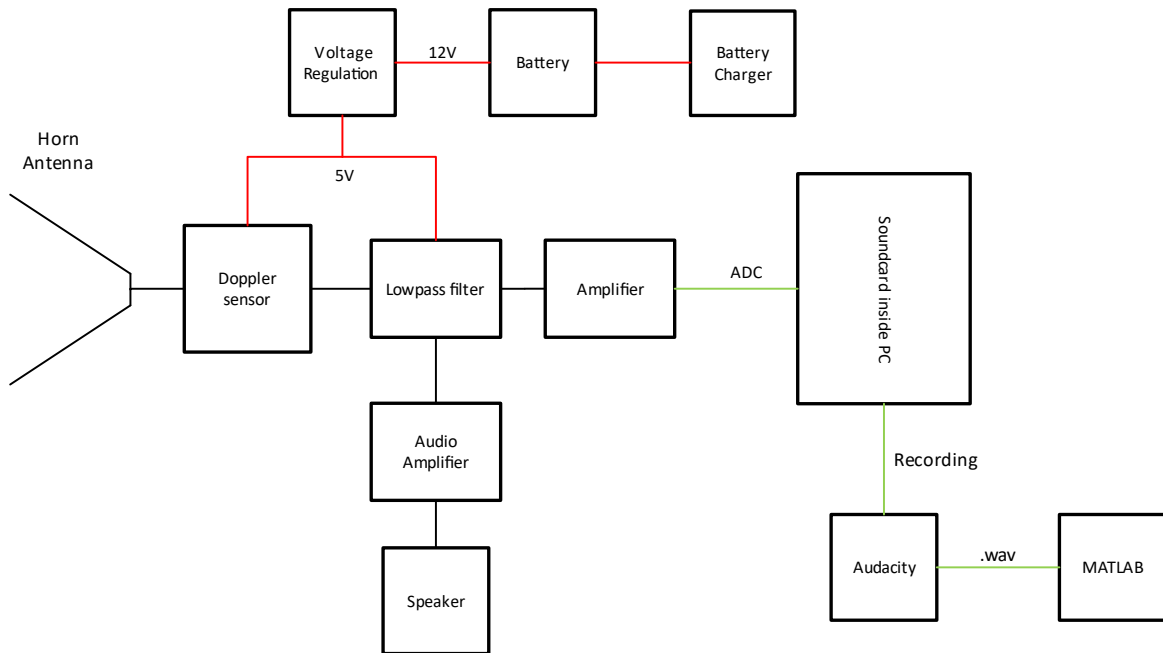


Figure 5.1: System Diagram of Project

5.1.1. Doppler Sensor

The Doppler sensor I will make use of for sensing the Doppler frequency is the HB100 [6]. The sensor operates at 10.525 GHz and is designed for velocity measuring. The sensor includes an oscillator, mixer, and transmit and receive antenna. The sensor can be operated in CW or FMCW mode. The radiation pattern of HB100 is illustrated in Figure ??, and the half power beamwidth is illustrated in Figure ???. The sensor requires a lowpass filter and pre-amplifier before it can be sampled for analysis, this is discussed in Section 5.1.3. Another option I considered was to build a sensor from individual components, but this proved to be too expensive and not within the scope of this project.

5.1.2. Antenna

The patch antenna on the HB100 sensor is shown in Figure 5.2. After looking at the radiation pattern I decided to design a horn antenna to increase the directivity of the antenna. A horn antenna, illustrated in Figure 5.3, was designed in CST software to act as a directional antenna for the patch antenna. Most of the details needed for the design of a horn antenna can be obtained from aperture theory [15].

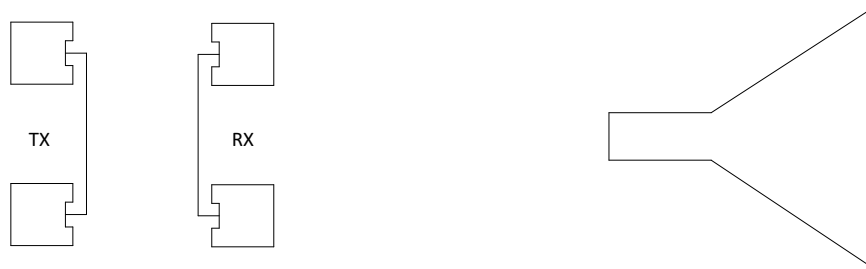


Figure 5.2: Patch Antenna on HB100

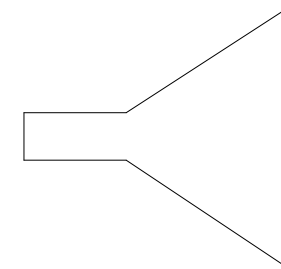


Figure 5.3: Horn Antenna

5.1.3. Lowpass Filter and Amplifier

The lowpass filter will be a second-order RC circuit, due to its simplicity and further filtering can be done in software. Active filters were considered but did not provide any advantage over a passive filter. The amplification of the sensor output proved to be a bit more ambitious. Due to little information available on the HB100 sensor and the uncertainty of the output voltage. The only information about output levels, where that it is in the range of a few mV [16]. The amplification will be tested and adapted as needed to sufficiently amplify the signal. To protect the soundcard of a laptop which has ADC voltage limits of 1 V_{rms} , the output signal needs to be clipped through a diode clipper circuit at 1 V. The functional block diagram is illustrated below.

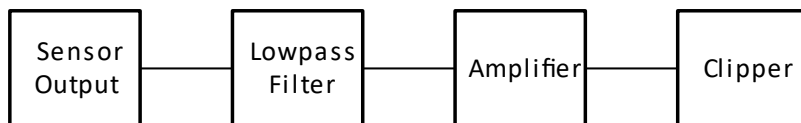


Figure 5.4: Functional Block diagram

5.1.4. Voltage Regulator

The choice of power supply is a linear voltage regulator. Another considered option was a switched-mode power supply. Switched mode power supply has a couple of advantages over linear voltage regulators, but it produces significantly more noise compared to linear voltage regulators. The noise might affect the HB100 sensor and due to the advantages

of switched mode not being utilized in my project, I decided to go with linear voltage regulators.

5.1.5. Soundcard

The soundcard inside a PC will be used to sample the Doppler sensor. The soundcard is capable of sampling at a range of frequencies from 8 kHz to 44 KHz. The Doppler frequency that I expect to sample will not exceed 6 kHz. The input limit is around 1 V_{rms} and thus the amplification is designed with this limitation taken into account.

5.1.6. Software

The sampled signal from the soundcard will be recorded in Audacity [17], which is open-source audio software. The recorded file will then be exported as a .wav file and further analyzed in MATLAB. In MATLAB I will apply software techniques to determine vehicle speed, and noise levels and apply them to track the vehicle. A GPS unit will be placed inside the car used for testing the system which will help with calibrating the system and used for comparison in non-ideal conditions. The GPS unit is a Ublox, GNSS smart board [18], with an external antenna to improve accuracy. The NMEA data strings that will be recorded in the Ublox software, will be copied to a text file and the speed extracted in MATLAB.

5.2. Detailed Design

5.2.1. Filter

Due to the low operating frequency expected from the Doppler sensor, I decided to use a second-order RC filter to get better attenuation at higher frequencies. The filter circuit is illustrated in Figure 5.5, and the cut-off frequency is calculated by equation 5.1. The cut-off frequency is selected as 8 kHz. This is quite a high cut-off frequency considering the expected output not to exceed 3 kHz. The choice for a second-order RC filter is chosen since the filter circuit has a gain that equals 0.707^n , where n equals the number of stages. The gain will therefore be 0.5 and thus I don't want to attenuate the necessary signals that I intend to measure. The values of the resistors and capacitors are chosen to be equal, R₁=R₂ and C₁=C₂. The capacitor value is chosen to be 10 nF, the calculated resistor value is 1.06 kΩ.

$$f_c = \frac{1}{2\pi\sqrt{R_1C_1R_2C_2}} \quad (5.1)$$

As the filter stage and therefore the roll-off slope increases, the low pass filters -3 dB

corner frequency point and therefore its pass band frequency changes from its original calculated value above by an amount determined by the following equation

$$f_{-3dB} = f_c \sqrt{2^{\frac{1}{n}} - 1} \quad (5.2)$$

The newly calculated cut-off frequency $f_c = 9.653$ kHz. The new cut-off frequency still satisfy the 6 kHz requirement.

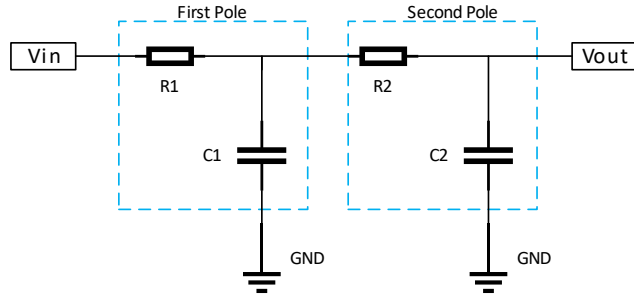


Figure 5.5: Filter Circuit

5.2.2. Amplifier

To amplify the output from the Doppler sensor, to be sampled by the PC soundcard the circuit is designed to be variable in the field. Therefore I decided to amplify the signal through a differential op-amp. The op-amp gain equation is shown below

$$V_{OUT} = \frac{R3}{R2} \times (V_b - V_a) \quad (5.3)$$

The amplifier is illustrated in figure 5.2.2, resistor R3 will be a variable resistor, known as a rheostat, R2's size is 1 kΩ. Thus a variable resistor that ranges up to around 470 kΩ is used, which will allow for a gain of up to 470. From the datasheet of the op-amp I used, MCP602 [19], the gain versus frequency plot is illustrated in figure C.1. The gain settles at 60 dB, which equals a gain of 1000, then starts to fall off at 1 MHz. The expected frequency should range from 1 to 3000 Hz, so the gain specifications can be met with one op-amp.

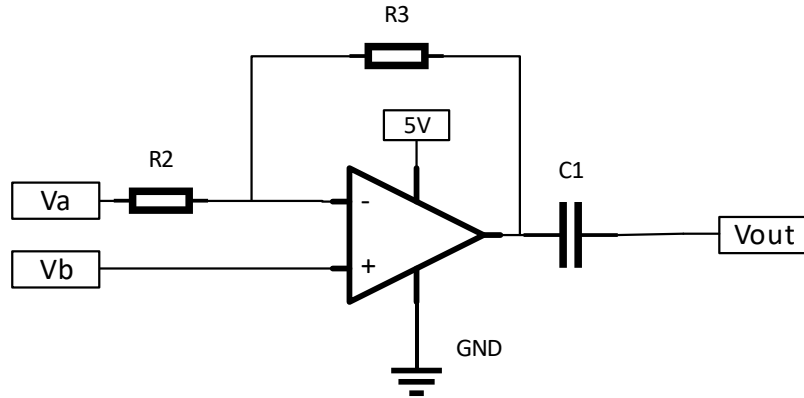
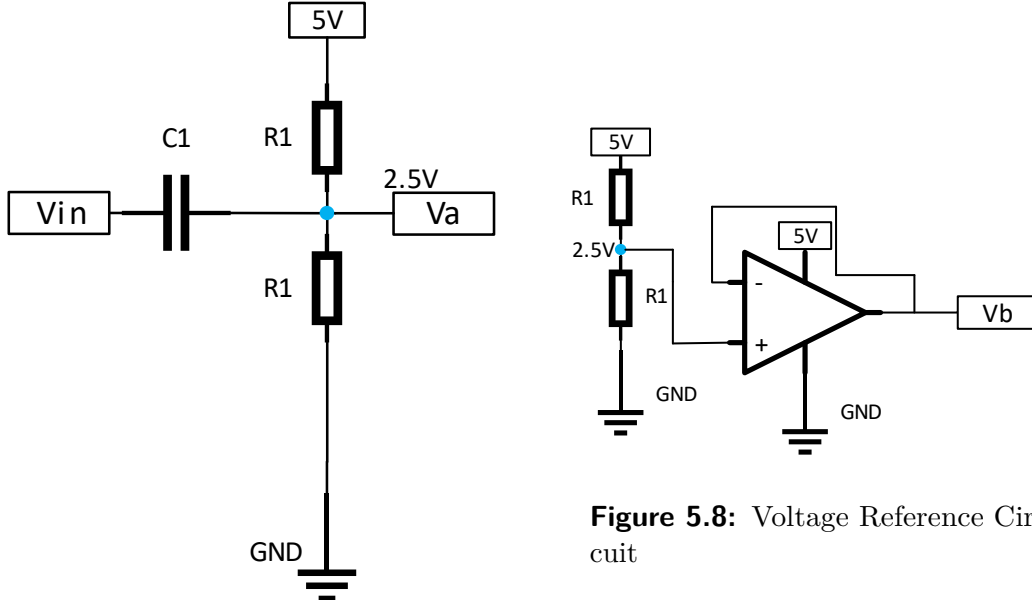


Figure 5.6: Amplifier Circuit

The voltage labels V_a and V_b , will both be centred around 2.5 V. This was chosen to give optimal swing on the output of the op-amp. The output will also swing around 2.5 V. The common mode input limits of the MCP602 op-amp ranges from $V_{ss}-0.3$ to $V_{DD}-1.2$, with $V_{ss}=0$ and $V_{DD}=5$, the limits ranges from -0.3 to 3.8. Therefore 2.5 V safely lies between the common mode voltage limits. The circuit required to produce voltage V_a is illustrated in 5.7, a decoupling capacitor is placed between the output voltage from the filter and the 2.5 V DC voltage that the AC will swing around. The voltage node between the two resistors is calculated by the equation below

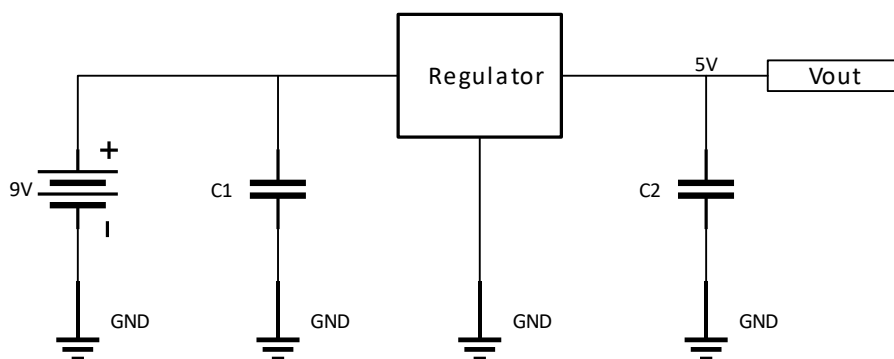
$$V_{ref} = 5 \times \frac{R1}{2 \times R1} = \frac{5}{2} \quad (5.4)$$

the value of $R1$ does not matter as long as the resistors are equal in size. The values are thus chosen to limit current and are $100\text{ k}\Omega$. A voltage follower is added between V_{ref} and V_b reference to stabilize the 2.5 V as the output swings, illustrated in figure 5.8. Voltages V_a and V_b are attached to the same labels in the circuit illustrated in figure 5.6.

**Figure 5.7:** Voltage Swing Circuit**Figure 5.8:** Voltage Reference Circuit

5.2.3. Voltage Regulator

The regulator circuit for generating 5 V is illustrated in figure 5.9. Capacitor C_1 is placed to help with input stability and C_2 is placed to help with the transient response. It is important to use a low noise voltage regulator to limit noise in the circuit. I used an LM7805 regulator [20]. The input voltage will be 12 V coming from an alkaline battery [21]. The expected output current will not exceed 200 mA. The power dissipated by the voltage regulator is 1 W and therefore there is no need for a heat sink or to do thermal calculations.

**Figure 5.9:** Voltage Regulator Circuit

5.2.4. Clipper

The clipper circuit is designed to limit the voltage swings at $\pm 1V$. This is achieved with a diode clipper circuit illustrated in figure 5.10. Two diodes are both placed with different

polarity facing V_{in} , this will clip the voltage level at the forward voltage drop of the diodes. After testing different diodes the forward voltages were around 0.5 V. It decided to place four diodes in the circuit with two of them having the same polarity. This limits the voltage swings at $\pm 1V$.

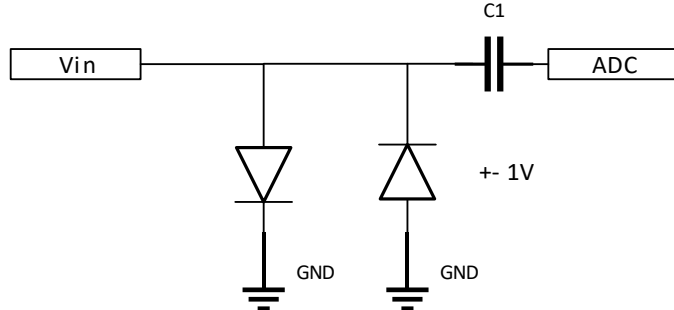


Figure 5.10: Diode Clipper Circuit

5.2.5. Antenna

To increase the range of the radar a horn antenna is used to increase the directivity of the *HB100* patch antenna. By focusing the radiation into a narrower band. This will increase the gain of the antenna and by looking back to equation 3.11, this will result in the increasing of measurable range. The first part of a horn antenna is a waveguide. The waveguide act as a feed for the signal propagating from the patch antenna into the horn. Figure 5.11 illustrates the shape of a rectangular waveguide. The main modes of propagation in the waveguide is either Transverse Electric Mode(*TE* mode) or Transverse Magnetic Mode(*TM* mode). TE_{mn} is used to represent the mode of propagating in the waveguide. The electromagnetic fields corresponding to the modes are shown below,

$$H_{zmn}(x, y, z) = h_{mn} \cos \frac{m\pi x}{a} \cos \frac{n\pi y}{b} e^{-jk_z z} \quad (5.5)$$

$$E_{zmn}(x, y, z) = e_{mn} \sin \frac{m\pi x}{a} \sin \frac{n\pi y}{b} e^{-jk_z z} \quad (5.6)$$

The TE_{10} is the dominant waveguide in the rectangular waveguide. But there are infinite TE_{mn} modes, but $m \neq n$. The width a and height b parameters are used for designing the cut off frequency of the waveguide.

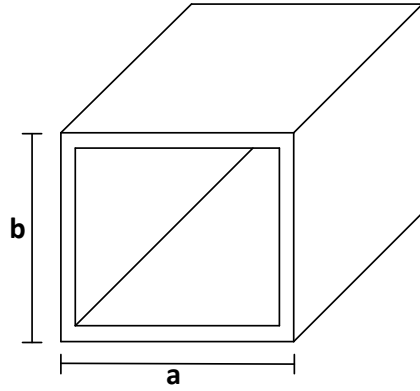


Figure 5.11: Rectangular Waveguide

The equation for calculating the cut off frequency is shown below,

$$f_{cmn} = \frac{c}{2\pi} \sqrt{\left(\frac{m\pi}{a}\right)^2 + \left(\frac{n\pi}{b}\right)^2} \quad (5.7)$$

Considering TE_{10} mode the equation is simplified to

$$f_{c10} = \frac{c}{2a} \quad (5.8)$$

Figure 5.12 illustrates the geometry of a horn antenna. The input waveguide can be any either rectangular or circular. Both options was simulated in CST and was selected.(reference the radiation pattern). W is the width of a rectangular aperture, and a is the radius of a circular aperture. The distance from the junction of the projected sides to the aperture is the slant radius R .

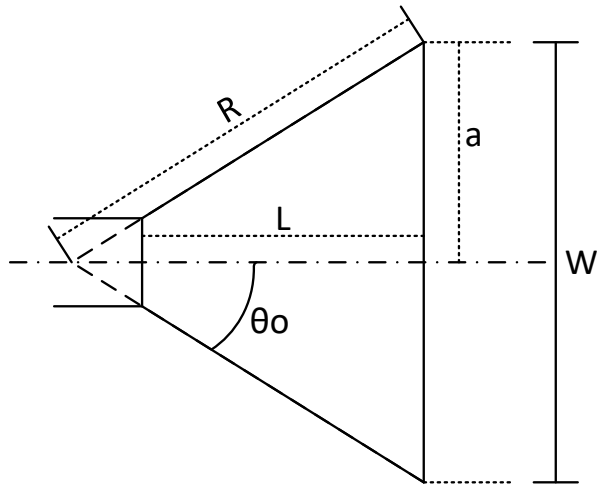


Figure 5.12: Horn Geometry

The dimensionless constant S is represented by

$$S = \frac{W^2}{8\lambda R} = \frac{a^2}{2\lambda R} \quad (5.9)$$

After simulation in CST, the dimensions for was chosen. the radiation pattern is show in figure.(in appendix).

5.2.6. Software

The common signal processing technique used in radars is to determine the strongest frequency component in a short period, through an STFT. This frequency component is then converted to speed. The speed calculation is designed to imitate that of real radar processing. The algorithm takes as inputs the recorded file, sampling rate, frame size, overlap size and signal-to-noise ratio(SNR). The algorithm is illustrated in algorithm 4.1. The output of the file will be an array with the speeds measured from the strongest frequency component of the signal in that short period.

The SNR level is calculated dynamically on each iteration of an STFT. This dynamically changes the level of the SNR, which leads to a better estimate of targets. This also improves the speed algorithms, capability when the radar is placed in different measurement locations. This is also the standard calibration, to determine the SNR of the location, when a permanent radar is installed in the field. The SNR algorithm is illustrated in algorithm 4.2. An example of an SNR is illustrated in figure D.1, where the red line is the SNR level. All the components above this line are measured as targets.

Algorithm 4.3 is to track a vehicle. This entails establishing a vehicle and tracking its speed for as long as it is in range of the radar. The algorithms ability to track a vehicles. The algorithm will assume only one vehicle will be in the range of the radar or in other words only try to track one vehicle. The STFT time period is used to determine the assumed maximum change in speed a vehicle can exercise. This speed variation is then used to set up bin ranges in the frequency domain. When the following STFT is calculated and a target is identified within these limits the new target frequency is used to update the bin ranges. This process repeats until the target falls outside of the range of the bins, meaning the target is out of range or possibly not the same vehicle. The measurable change in the speed of a vehicle is directly proportional to how long the period is used to calculate the STFT. Equation 5.10 shows how this speed change can be calculated if the radar will have 100 % accuracy in speed changes.

$$\text{Speed} = \frac{1}{t_i} \quad (5.10)$$

gensymb

Chapter 6

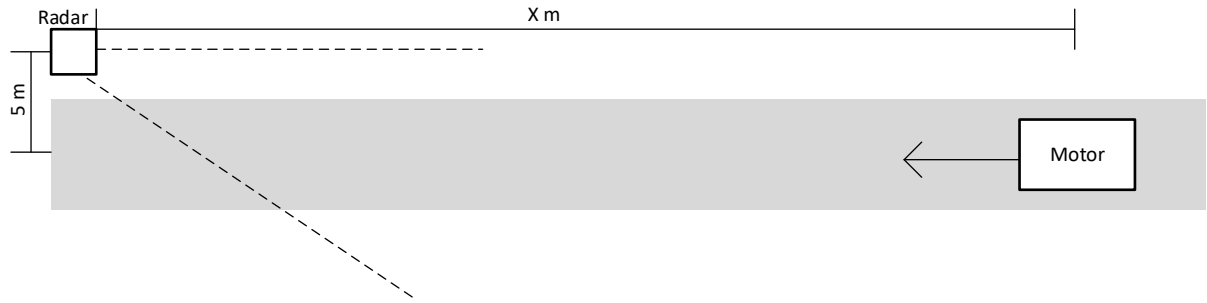
Results

6.1. Radar and Setup



Figure 6.1: Caption

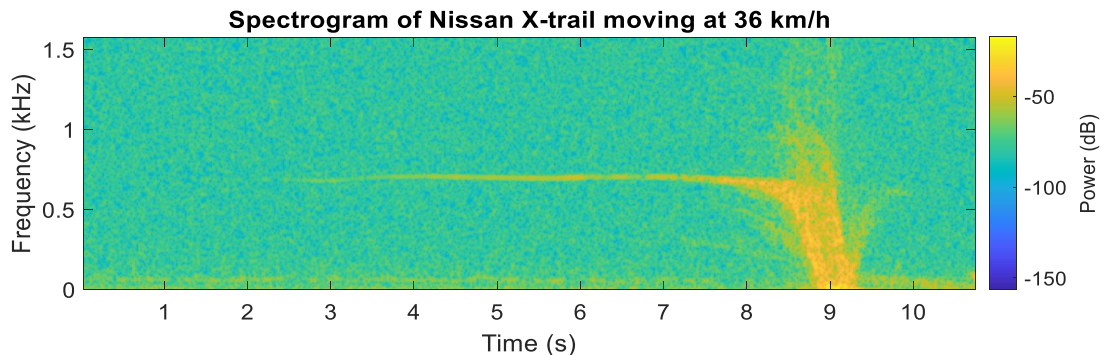
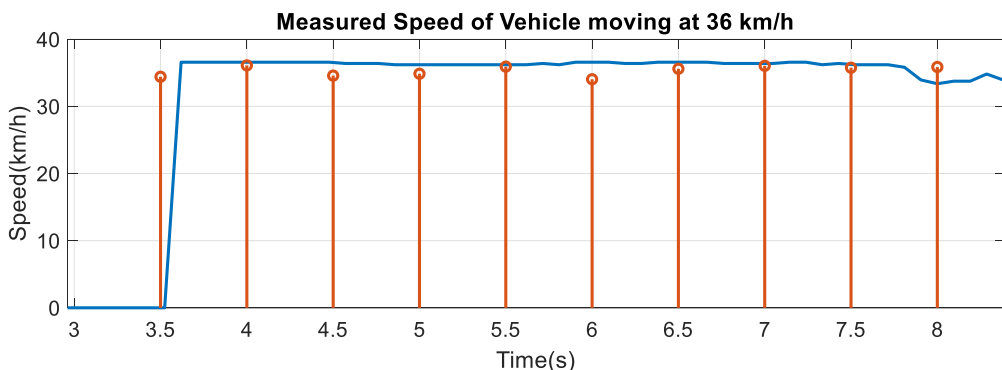
Illustrated above is the structure and hardware of the radar. The radar is built around a wooden structure that imitates that of a real radar speed trap. The radar will be placed next to a road located at 5 m from the center. The radar will be pointed at the oncoming motors. The motor used for testing will be a Nissan X-trail, that will be put on cruise control. Inside the car the GPS unit will be placed that will also log the NMEA data of the motor for speed comparison(show photo in appendices). The setup is illustrated in figure 6.2.

**Figure 6.2:** Radar Setup

6.2. Radar Results

The radar designed in Chapter 5, was simulated in LTSpice. The circuits are illustrated in figure F.1. Figure F.2 illustrate the workings of the amplification circuit. Figure F.3, illustrates the frequency response of the 8 kHz cut-off lowpass filter.

Figure 6.3 illustrates the spectrogram of a Nissan X-trail moving at 36 km/h with cruise control on. The spectrogram clearly indicates when the radar sees the target, the yellow line around 700 Hz. Figure 6.4 illustrates the tracking algorithm applied to the signal. Alongside the radar speed measurement the GPS speed is also plotted for comparison. The radar and its software is capable of measuring a vehicles speed accurately.

**Figure 6.3:** Spectrogram of Nissan X-trail traveling at 36 km/h**Figure 6.4:** Speed Extraction from STFT

6.3. Limitations and Operation

6.3.1. Results of Cosine Effect

Section 4.1 explains the cosine effect. As concluded in that section, the measured speed will always be less than the real speed of a vehicle. In two the cases where d is equal to 3 m and 6 m. The speed measured by the radar is shown in blue. By knowing the maximum distance that the radar is capable of measuring a vehicle. Software can be used to estimate and correct the cosine error. The corrected cosine error for both distances are illustrated in the figure below. Note that when the vehicle is within 3 to 5 m of the radar, the speed of the vehicle is no longer measurable due to saturation. Consequently the cosine error gives false corrections. This phenomenon is discussed in section 6.3.6.

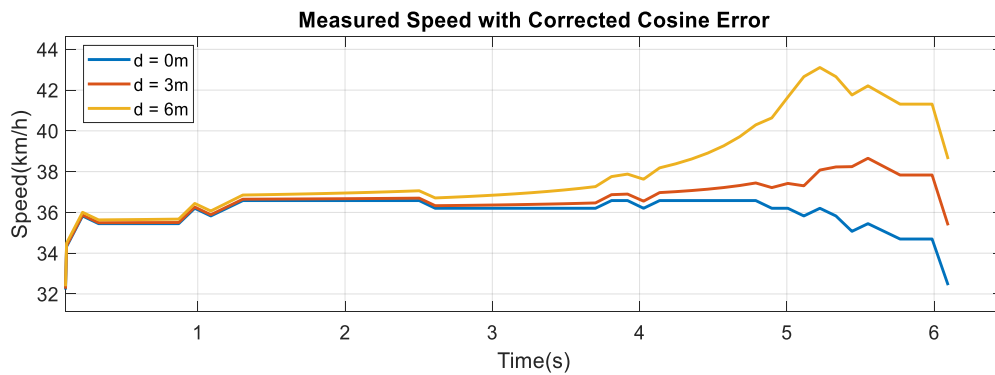


Figure 6.5: Cosine Error on Vehicle Speed

Despite that the cosine error is capable of being corrected. The operation and setup of a radar is very important. For the radar is not capable of determining in what lane the vehicle will be travelling. This will mean that the radar cannot correct the cosine error on more than one lane at a time. The cosine error can only be corrected where the distance d will remain the same for all vehicles passing by the radar. Multiple lane application will results in erroneous measurements.

6.3.2. Results of Accuracy and Acceleration Limits

The configuration of the DFT sample size is important for the accuracy of a radar as mentioned in Section 4.2. To illustrate this phenomenon Figure 6.6 is an indication of a correctly set up DFT. The measurement is of a vehicle accelerating past the radar. The radar accurately calculates the acceleration of the vehicle without to many calculations. The accompanying spectrogram is shown in figure G.1.

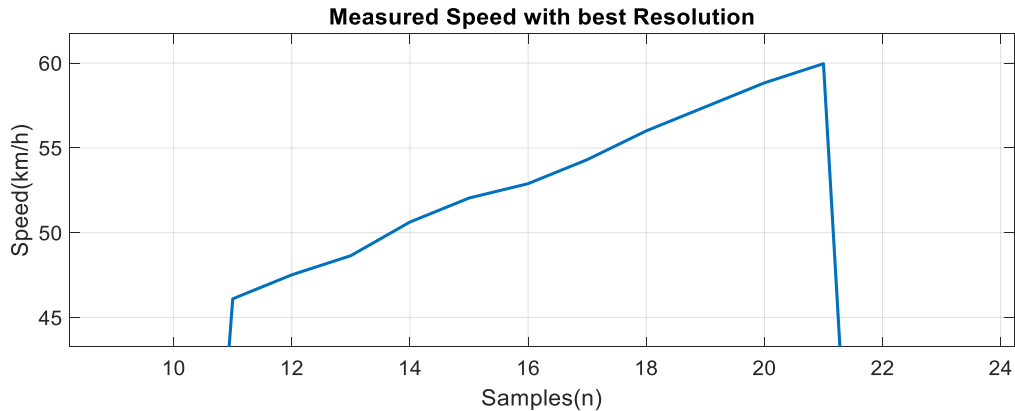


Figure 6.6: Measured Speed with best combination of Time and Frequency Differentiation

When the DFT sample size is set too big. The radar is incapable of calculating the change in speed. This is illustrated in figure 6.7. The measured speed is not an accurate estimate of the accelerating vehicle. The change in speed per sample is around 4 km/h which does not satisfy the required accuracy for a radar. The accompanying spectrogram, illustrated in figure G.2, clearly indicates how the radar is capable of differentiating between frequency components, but unable to differentiate in time.

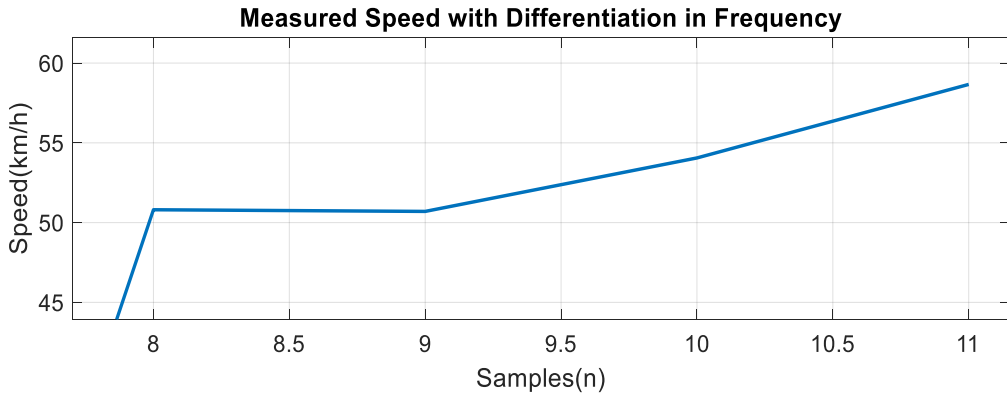


Figure 6.7: Measured Speed with Differentiation in Frequency

If the DFT sample size is too small. The radar is measuring the acceleration accurately but there are too many measurements. This will require powerful processing which is unnecessary. Some of the measurements recorded the same speed as the previous measurement. In comparison to figure 6.6, which requires 10 samples, figure 6.8 calculates 25 samples. The accompanying spectrogram is shown in figure G.3. The spectrogram is a clear indication of how the frequency differentiation is lost when time differentiation is prioritised.

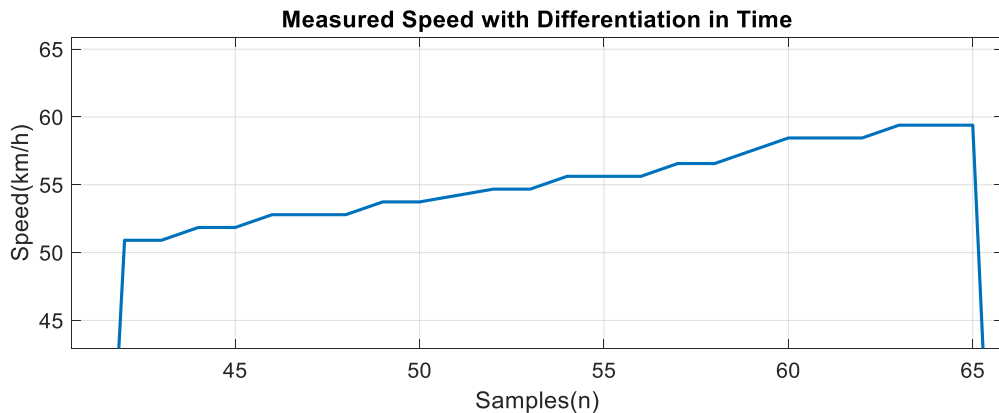


Figure 6.8: Measured Speed with Differentiation in Time

6.3.3. Results of Object Identification

6.3.4. Results of Antenna Sidelobes

To demonstrate the effect of antenna sidelobes, the radar will be rotated from north to indicate the importance radiation and radar setup can have on the readings.

Table 6.1: Measurable Distance of Radar

Degrees West of North	HB100 Antenna	Horn Antenna
0°	56.08m	tbc
20°	51.57m	tbc
40°	29.55m	tbc

6.3.5. Results of Multiple Path Reflection

6.3.6. Results of Radar Receiver Saturation

As discussed in Section 4.6, the radar is subject to saturation whenever a vehicle drives closely by the radar. This will cause a moment where the radar will be blind to any other moving vehicles in the range. Depending on how the radar is set up. If vehicles are coming from the opposite direction the radar is pointing in. This will cause the radar to unexpectedly lose its visibility. Figure 6.9 illustrates the spectrogram of two vehicles, one moving towards the radar from the direction it is pointing in and one vehicle moving in the opposite direction. The distortion causes the radar to lose track of the first vehicle for a moment. The radar is then locked on to the second vehicle until the first vehicle passes by the radar and the phenomenon occurs again.

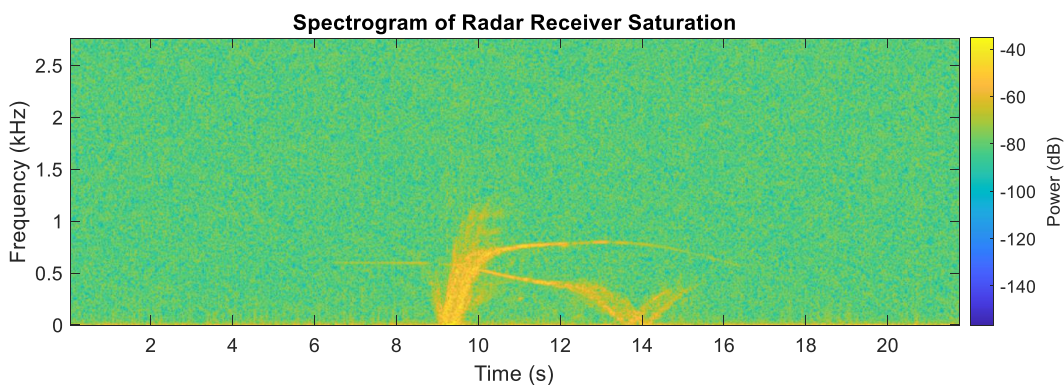


Figure 6.9: Spectrogram of Radar Receiver Saturation

The tracking software applied is shown in figure 6.10. The graph clearly illustrates when there is a vehicle passing by the radar and where the radar is and is not capable of tracking a vehicle.

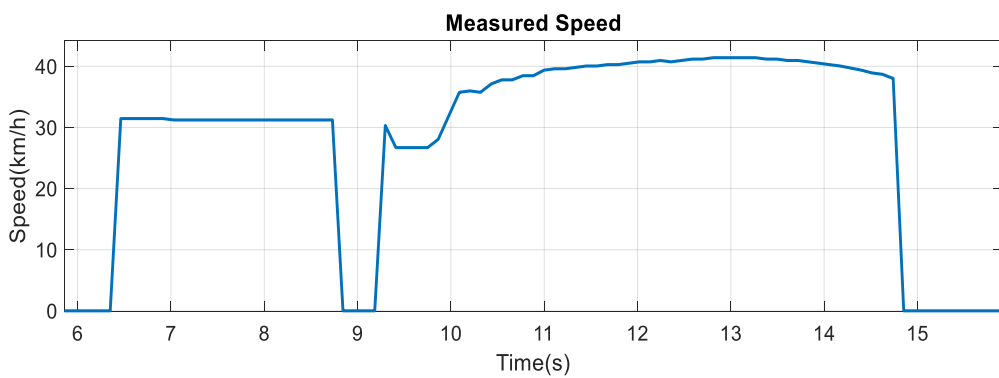


Figure 6.10: Speed tracking when Saturation occurs

Chapter 7

Conclusion

Bibliography

- [1] Sutori, “The doppler effect.” [Online]. Available: <https://www.sutori.com/en/item/untitled-420a-4b20>
- [2] , “The catalina preservation society.” [Online]. Available: <https://pbycatalina.com/specifications/>
- [3] B. van der Riet, “An investigation of the integrity of the doppler radar measurement of vehicle speeds, with particular reference to the digidar 1-k instrument.”
- [4] N. C. Martin, “A microwave doppler technique for vehicle speed determination,” Masters Thesis, University of Cape Town, Rondebosch, Cape Town, 7700, 1987.
- [5] N. G. Lam, “Vehicle speed measurement using doppler effect,” Honours Thesis, VAASAN AMMATTIKORKEAKOULU UNIVERSITY OF APPLIED SCIENCES, Wolffintie 30, 65200 Vaasa, Finland, 2021.
- [6] *X-Band Microwave Motion Sensor Module Application Note*, ST Electronics, May 2018, rev. 1.
- [7] M. I. Skolnik, *INTRODUCTION TO RADAR SYSTEMS*. McGraw-Hill Book Co., 1981.
- [8] S. Farahani, “Rf propagation, antennas, and regulatory requirements,” *ZigBee Wireless Networks and Transceivers*, pp. 177–206, 2008.
- [9] I. T. Union, “Itu telecommunication standardization sector.” [Online]. Available: <https://www.itu.int/en/Pages/default.aspx>
- [10] K. S. INC., “Frequency information: K, ka, ku x bands.” [Online]. Available: <https://kustomsignals.com/blog/police-speed-radar-gun-frequency-information-k-ka-ku-x-bands>
- [11] A. E. Fuhs, “Radar cross section lectures,” Lectures, Monterey, California, Naval Postgraduate School, 411 Dyer Road, 1982.
- [12] P. R. I. Center, “Vehicle reflection.” [Online]. Available: <https://coprada.com/chapts/chapt3/ch3d6.htmls>
- [13] W. A. H. MARK A. Richards, James A. Scheer, *Principle of Modern Radar*. SciTech Publishing, 2010.

- [14] C. Wolff, “Radar basics.” [Online]. Available: <https://www.radartutorial.eu/01.basics/lrb02.en.html>
- [15] T. A. Milligan, *Modern Antenna Design*. John Wiley Sons, 2005.
- [16] J. Beale, “p=playing with cheap hb100 doppler radar module for car speed.” [Online]. Available: <https://www.eevblog.com/forum/projects/playing-with-cheap-hb100-doppler-radar-module-for-car-speed/>
- [17] “Audacity.” [Online]. Available: <https://www.audacityteam.org/>
- [18] *NEO-M8 u-blox M8 concurrent GNSS modules*, Ublox, Oct. 2021, rev. 1.
- [19] *2.7V to 6.0V Single Supply CMOS Op Amps*, Microchip, Oct. 2007, rev. 1.
- [20] *μ A7800 SERIES POSITIVE-VOLTAGE REGULATORS*, Texas Instruments, May 1976, rev. 1.
- [21] *12V Alkaline Battery*, RS PRO, Oct. 2022, rev. 1.

Appendix A

Project Planning Schedule

This is an appendix.

Appendix B

Outcomes Compliance

This is another appendix.

Appendix C

Figures

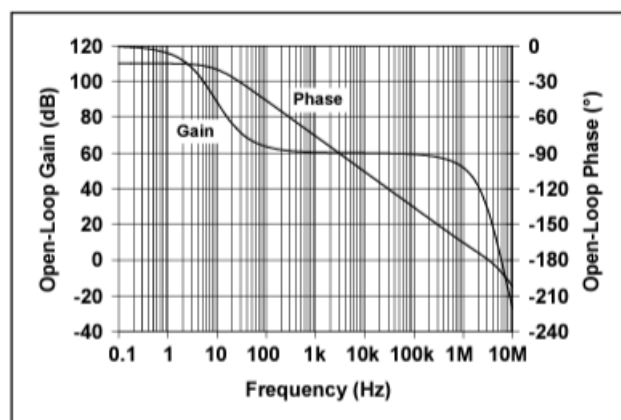


Figure C.1: Gain versus Frequency plot of MCP602 op-amp

Appendix D

Radar Software

Algorithm 4.1: Speed

input Recording, Sampling Rate, Frame Size, Signal-to-Noise Ratio
for $n = 0$ to $frames$ **do**
 Calculate FFT of sample
 Calculate maximum frequency component
 Store frequency component in array
for $n = 0$ to $frames$ **do**
 Convert frequency component to speed
 Plot speed versus time

Algorithm 4.2: Signal to Noise Ratio

input Recording, Sampling Rate, Frame Size
for $n = 0$ to $frames$ **do**
 Calculate FFT of Sample
for $i = 0$ to $SampleSize$ **do**
 Summation of Frequency Components
 Store SNR per frame
SNR = Summation of SNR per frame divided by total frames
output Signal-to-Noise Ratio

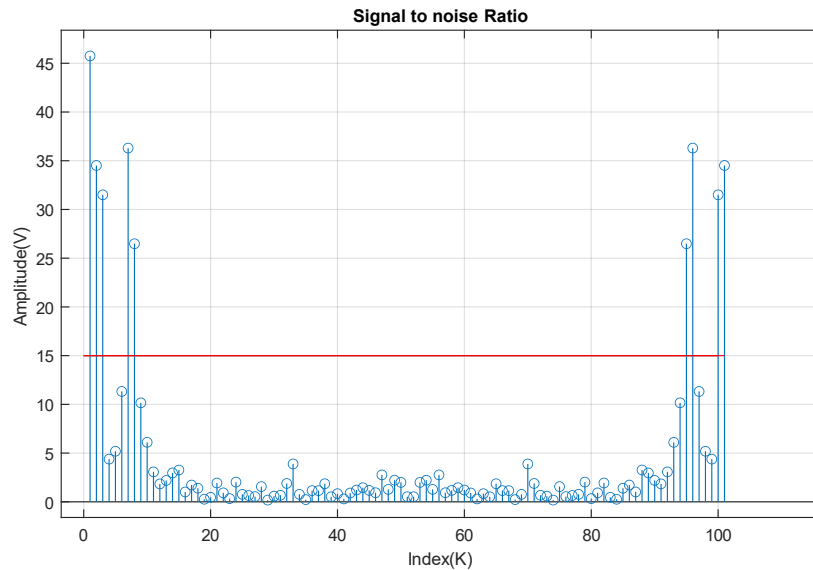


Figure D.1: Signal-to-Noise Ratio

Algorithm 4.3: Tracking

```

input Recording, Sampling Rate, Frame Size, Signal-to-Noise Ratio, Frequency Bin Size
for  $n = 0$  to  $frames$  do
    Calculate FFT of Sample
    for  $i = 0$  to  $SampleSize$  do
        Calculate Maximum Component
        if Maximum Component  $\geq$  SNR then
            if Frequency Difference  $\leq$  Bin Range then
                Label Object
                Update bin range
            Store Object Frequency
        Plot Tracked Object Speed vs Time
output Tracked Object Speed

```

Appendix E

Antennas

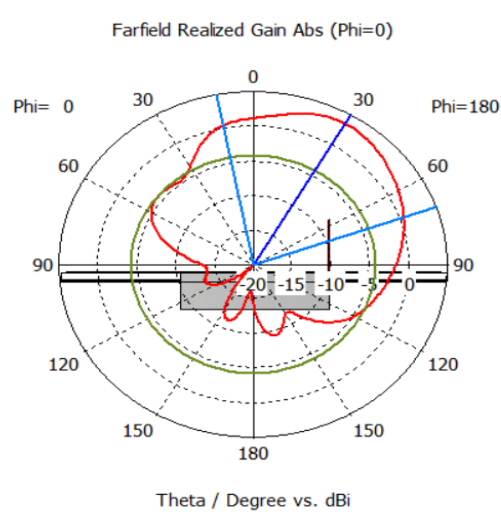


Figure E.1: HB100 Radiation Pattern in CST

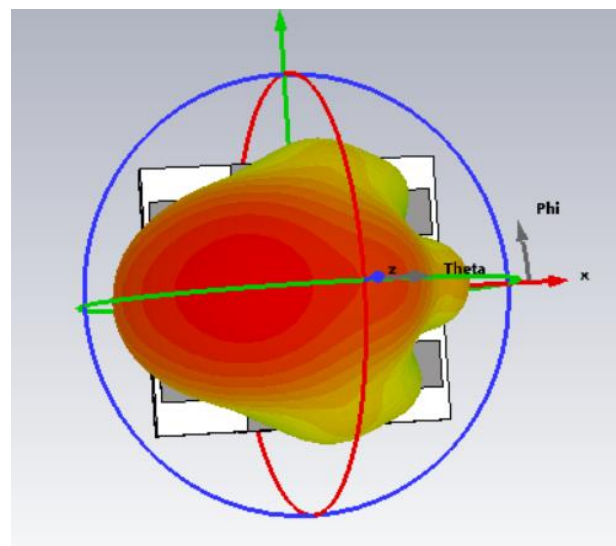


Figure E.2: HB100 3D Radiation Pattern in CST

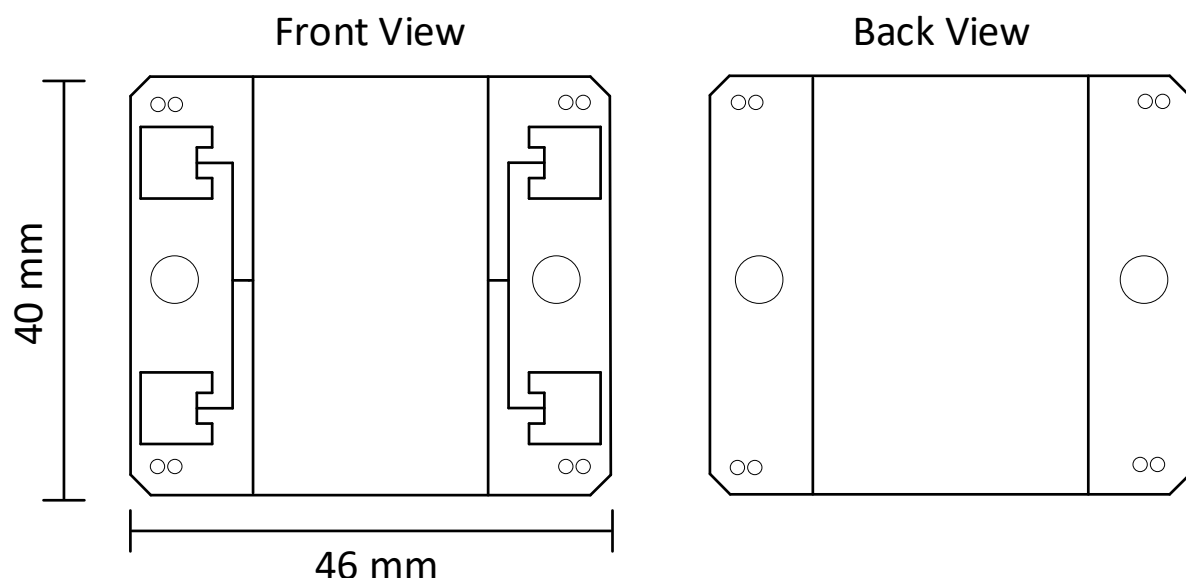


Figure E.3: Schematic Drawing of HB100 Sensor

Appendix F

LTS spice Simulations

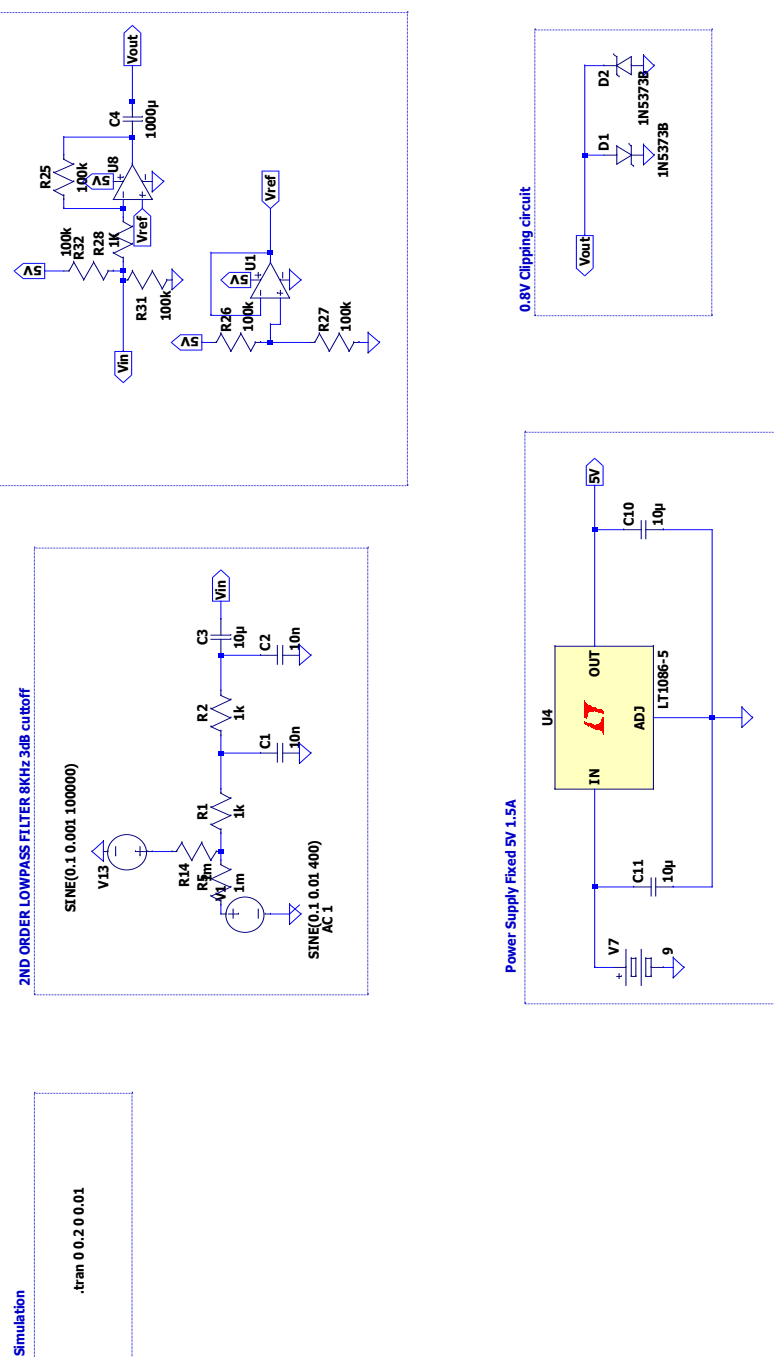


Figure F.1: LTSpice Simulation of Radar Hardware

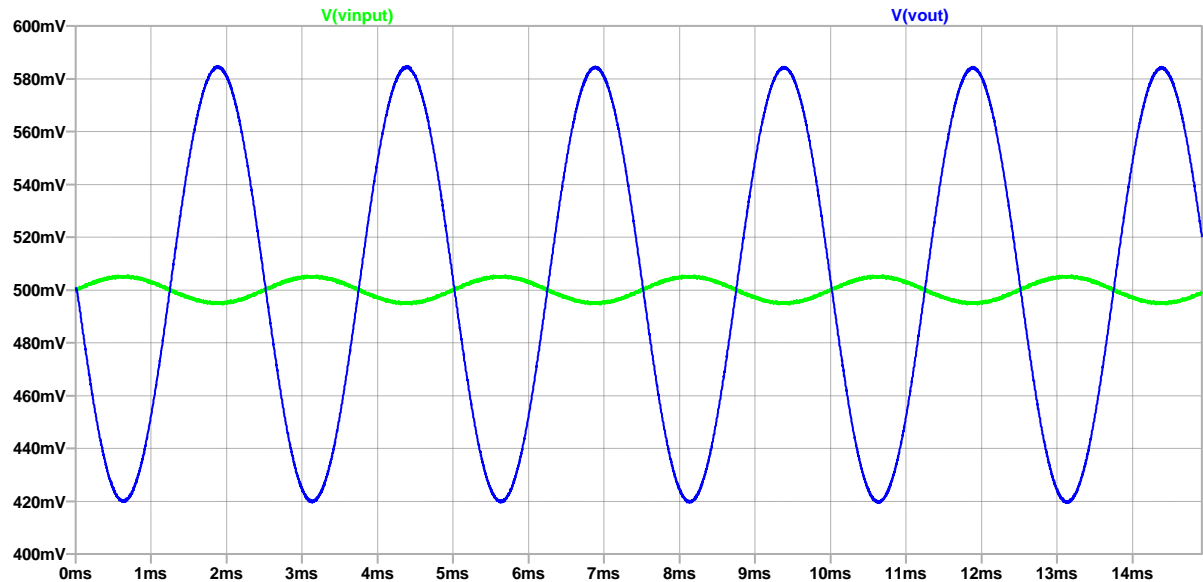


Figure F.2: Input and Amplified Output

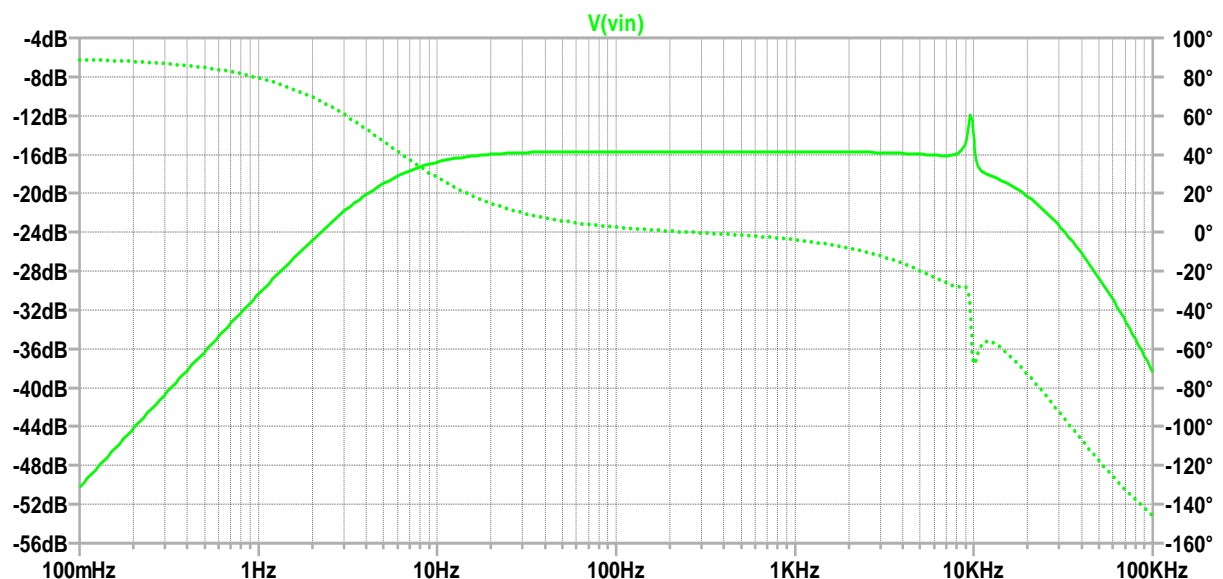


Figure F.3: Frequency Response of Lowpass Filter

Appendix G

Spectrogram regarding Accuracy and Acceleration

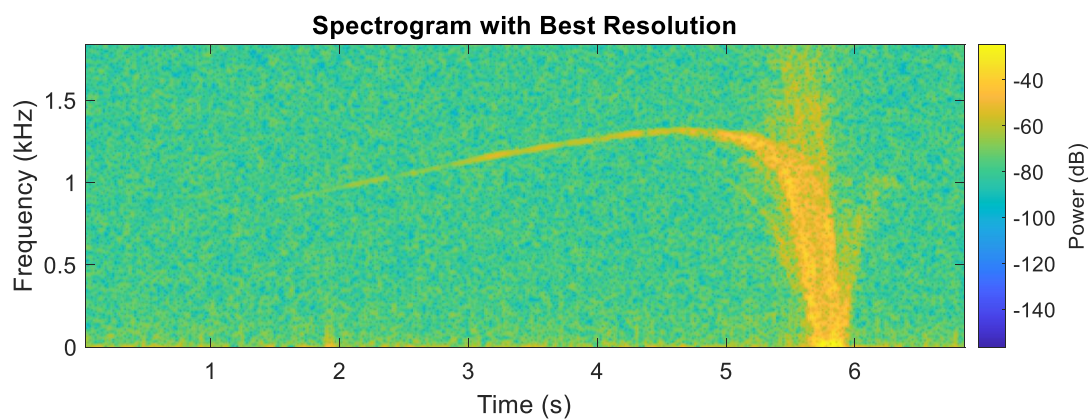


Figure G.1: Spectrogram with best combination of Time and Frequency Resolution

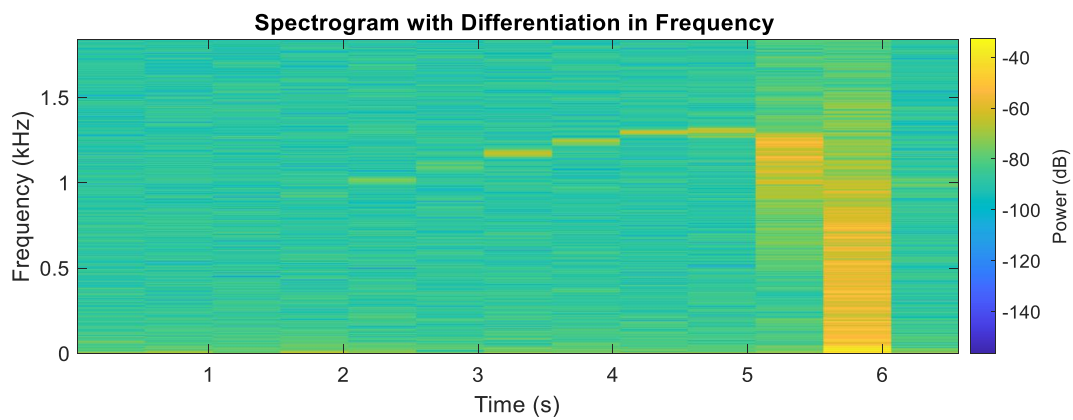


Figure G.2: Spectrogram with Differentiation in Frequency

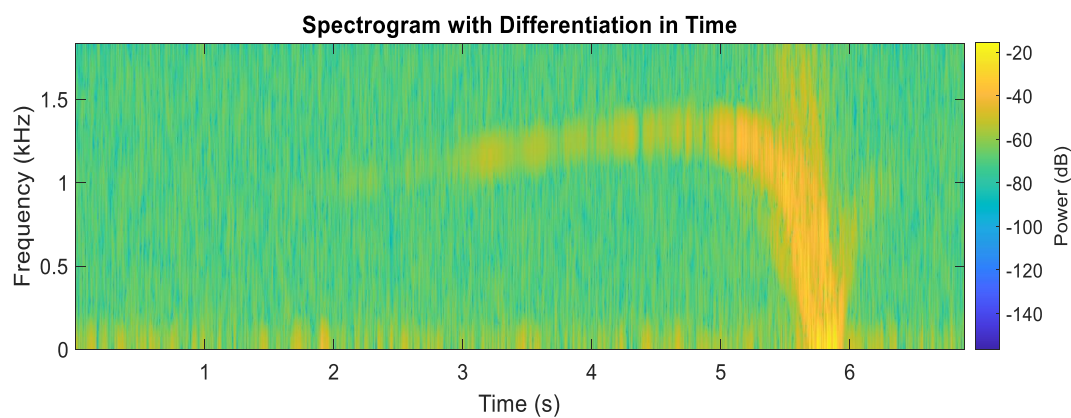


Figure G.3: Spectrogram with Differentiation in Time

Appendix H

Spectrograms regarding Antenna Sidelobe

The spectrograms below are from measurements with the HB100 sensor before adding the horn antenna. Take note of the radiation pattern of the HB100 antenna, illustrated in figure ??.

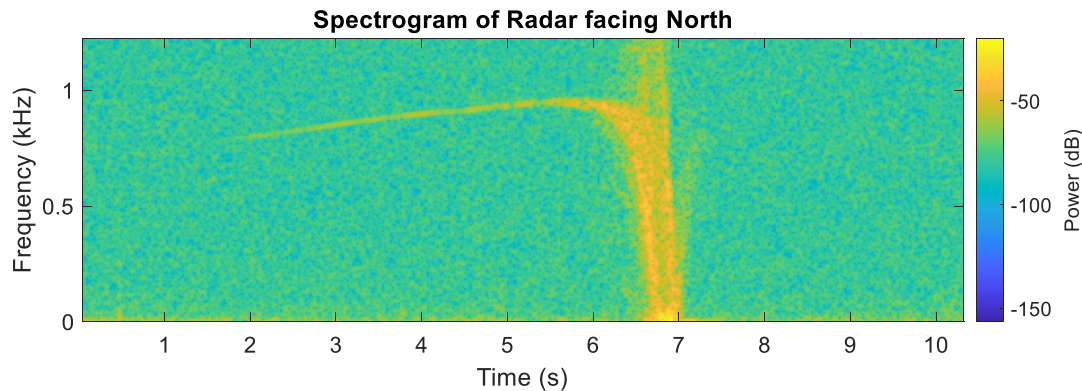


Figure H.1: Caption

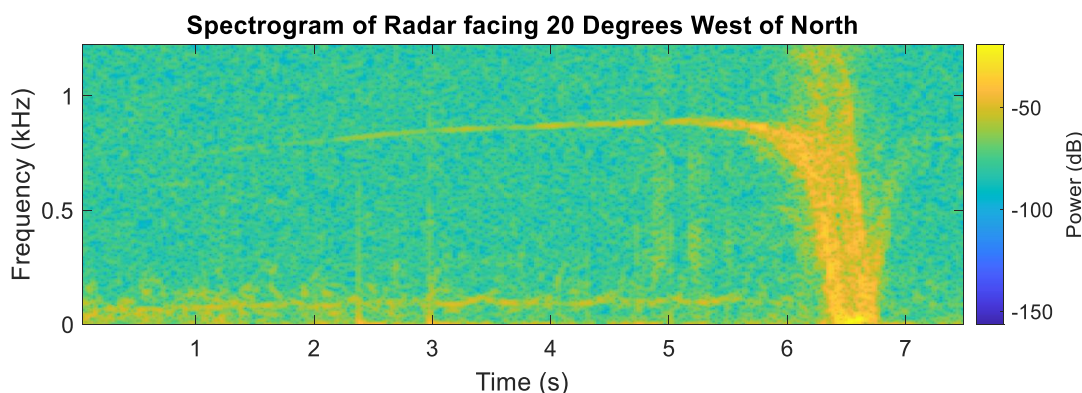


Figure H.2: Caption

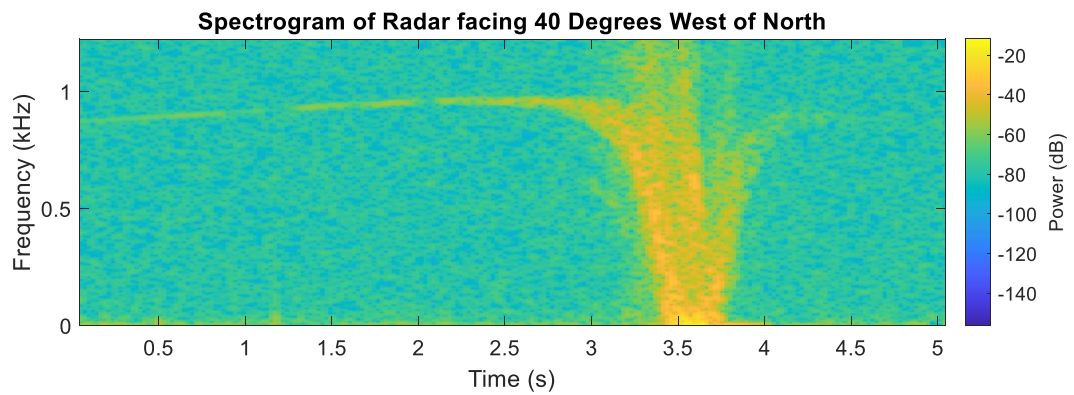


Figure H.3: Caption

The next set of spectrograms were measured after the adding of the horn antenna. The radiation pattern of the horn antenna added to the radar, is illustrated in figure ??.